

# QUANTUM FOAM, GRAVITY AND GRAVITATIONAL WAVES

**Reginald T. Cahill**

School of Chemistry, Physics and Earth Sciences  
Flinders University  
GPO Box 2100, Adelaide 5001, Australia  
Reg.Cahill@flinders.edu.au

To be published in  
**Relativity, Gravitation, Cosmology**

Abstract

The new information-theoretic Process Physics has shown that space is a quantum foam system with gravity being, in effect, an inhomogeneous in-flow of the quantum foam into matter. The theory predicts that absolute motion with respect to this system should be observable, and it is shown here that absolute motion has been detected in at least seven experiments. As well this experimental data also reveals the existence of a gravitational wave phenomena associated with the in-flow. It is shown that Galilean Relativity and Special Relativity are in fact compatible, contrary to current beliefs: absolute motion actually causes the special relativity effects. The new theory of gravity passes all the tests of the previous Newtonian and General Relativity theories, but in addition resolves the numerous gravitational anomalies such as the spiral galaxy 'dark matter' effect, the absence of 'dark matter' in elliptical galaxies, the inconsistencies in measuring  $G$ , the borehole  $g$  anomaly, and others. It is shown that Newtonian gravity is deeply flawed, because the solar system from which it was developed has too high a spherical symmetry to have revealed key aspects of the phenomena of gravity, and that General Relativity inherited these flaws. The data are revealing that space has structure, and so indicates for the first time evidence of quantum space and quantum gravity effects.

Keywords: Quantum foam, in-flow gravity, absolute motion, gravitational anomalies, gravitational waves, process physics.

# Contents

<b>1</b>	<b>Introduction</b>	<b>2</b>
<b>2</b>	<b>A New Theory of Gravity</b>	<b>4</b>
2.1	Classical Effects of Quantum Foam In-Flow . . . . .	4
2.2	The Einstein Measurement Protocol . . . . .	8
2.3	The Origins of General Relativity . . . . .	11
2.4	Deconstruction of General Relativity . . . . .	13
2.5	The New Theory of Gravity . . . . .	14
2.6	The ‘Dark Matter’ Effect . . . . .	16
2.7	In-Flow Superposition Approximation . . . . .	17
2.8	Gravitational In-Flow and the GPS . . . . .	18
2.9	Measurements of $G$ . . . . .	20
2.10	Gravitational Anomalies . . . . .	21
2.11	The Borehole $g$ Anomaly . . . . .	23
<b>3</b>	<b>Detection of Absolute Motion and Gravitational Waves</b>	<b>25</b>
3.1	Space and Absolute Motion . . . . .	25
3.2	Theory of the Michelson Interferometer . . . . .	25
3.3	The Michelson-Morley Experiment: 1887 . . . . .	29
3.4	The Miller Interferometer Experiment: 1925-1926 . . . . .	33
3.5	Gravitational In-flow from the Miller Data . . . . .	36
3.6	The Illingworth Experiment: 1927 . . . . .	38
3.7	The Joos Experiment: 1930 . . . . .	40
3.8	The New Bedford Experiment: 1963 . . . . .	41
3.9	The DeWitte Experiment: 1991 . . . . .	43
3.10	The Torr-Kolen Experiment: 1981 . . . . .	48
3.11	Galactic In-flow and the CMB Frame . . . . .	49
3.12	In-Flow Turbulence and Gravitational Waves . . . . .	50
3.13	Vacuum Michelson Interferometers . . . . .	52
3.14	Solid-State Michelson Interferometers . . . . .	52
3.15	Absolute Motion and Quantum Gravity . . . . .	53
<b>4</b>	<b>Conclusions</b>	<b>55</b>
<b>5</b>	<b>Acknowledgments</b>	<b>56</b>

## 1 Introduction

The new information-theoretic *Process Physics* [1, 2, 3, 4, 5, 6, 7, 8, 9] provides for the first time an explanation of space as a quantum foam system in which gravity is an inhomogeneous flow of the quantum foam into matter. That work has implied that absolute motion should be observable and that gravity is caused by an effective inhomogeneous in-flow of quantum-foam/space into matter. It

is shown here that Newtonian gravity and General Relativity may be re-written in a ‘fluid in-flow’ formalism, and that a simple generalisation of this formalism leads to a new theory of gravity, at the classical level, that is in better agreement with the experimental data. It passes all the standard tests of both the Newtonian and the General Relativity theories of gravity. Significantly this new theory of gravity is shown to resolve the many gravitational anomalies that have been reported - the spiral galaxy ‘dark matter’ effect, the absence of ‘dark matter’ in elliptical galaxies, the ongoing inconsistencies in measuring  $G$ , the borehole  $g$  anomalies and many others. These anomalies, as it is now becoming clear, were revealing deep flaws in the Newtonian and General Relativity formalisms. It turns out that Newtonian gravity is flawed because in its initial formulation the phenomena of the solar system were too special - the solar system has too much spherical symmetry to have revealed all the aspects of gravity. General Relativity, in turn, is seen to be also flawed, because it ‘inherited’ these flaws from the Newtonian theory. As well the new theory of gravity predicts a new kind a gravitational wave, essentially turbulence in the in-flowing space, and this phenomena is evident in the experimental data. As well it is shown that Galilean Relativity and the Lorentzian Relativity are actually consistent, and together describe real physical phenomena - until now they were regarded as mutually exclusive. Overall we see that the quantum foam system that is space is more complex and subtle than the models and paradigms of current physics. These developments indicate that we are seeing for the first time evidence of quantum space and quantum gravity effects - the experimental data is revealing that space has ‘structure’.

An analysis herein of data from seven experiments reveals that absolute motion relative to space has been observed by Michelson and Morley (1887) [10], Miller (1925/26) [11], Illingworth (1927) [12], Joos (1930) [13], Jaseja *et al.* (1963) [14], Torr and Kolen (1981) [15], and by DeWitte (1991) [16], contrary to common belief within physics that absolute motion has never been observed. The first five of these were Michelson interferometer experiments operating with a gas, while the last two were coaxial cable RF travel-time experiments using atomic clocks. Amazingly no-one had ever analysed the fringe shift data from the interferometer experiments using two well-known but overlooked key effects; namely the Fitzgerald-Lorentz contraction effect and the refractive index effect which slows down the speed of light in the gas. The Dayton Miller data also reveals the in-flow of space into the sun which manifests as gravity. The experimental data of Miller, DeWitte, and Torr and Kolen indicate that the in-flow manifests turbulence, which amounts to the observation of a gravitational wave phenomena.

Absolute motion is consistent with special relativistic effects, which are caused by actual dynamical effects of absolute motion through the quantum foam. The Lorentzian interpretation of relativistic effects is seen to be essentially correct. Vacuum Michelson interferometer experiments or its equivalent [18, 19, 20, 21] cannot detect absolute motion. The various gas-mode Michelson interferometer data cannot be analysed unless the special relativistic effects are taken into account, and indeed these experiments demonstrate the validity and

reality of the Fitzgerald-Lorentz contraction effect.

## 2 A New Theory of Gravity

### 2.1 Classical Effects of Quantum Foam In-Flow

We begin here the analysis that reveals the new theory and explanation of gravity. In this theory gravitational effects are caused solely by an inhomogeneous ‘flow’ of the quantum foam. The new information-theoretic concepts underlying this physics were discussed in [1, 2, 5]. Essentially matter effectively acts as a ‘sink’ for that quantum foam. It is important to realise that this is not a flow of ‘something’ through space; rather it is ongoing structural changes in space - a fluctuating and classicalising quantum foam, but with those changes most easily described as a ‘flow’, though such a flow is only evident from distributed observers. The Newtonian theory of gravity was based on observations of planetary motion within the solar system. It turns out that the solar system was too special, as the planets acted as test objects in orbit about a spherically symmetric matter distribution - the sun. As soon as we depart from such spherical symmetry, and even within a spherically symmetric matter distribution problems appear. Only the numerous, so-far unexplained, gravitational anomalies are actually providing clues as to the real nature of gravity. The Newtonian theory was originally formulated in terms of a force field, the gravitational acceleration  $\mathbf{g}(\mathbf{r}, t)$ , but as will be shown here it is much closer to the truth if we re-formulate it as a ‘fluid-flow’ system. The gravitational acceleration  $\mathbf{g}$  in the Newtonian theory is determined by the matter density  $\rho(\mathbf{r}, t)$  according to

$$\nabla \cdot \mathbf{g} = -4\pi G\rho. \quad (1)$$

For  $\nabla \times \mathbf{g} = 0$  this gravitational acceleration  $\mathbf{g}$  may be written as the gradient of the gravitational potential  $\Phi(\mathbf{r}, t)$

$$\mathbf{g} = -\nabla\Phi, \quad (2)$$

where the gravitational potential is now determined by  $\nabla^2\Phi = 4\pi G\rho$ . Here, as usual,  $G$  is the gravitational constant. Now as  $\rho \geq 0$  we can choose to have  $\Phi \leq 0$  everywhere if  $\Phi \rightarrow 0$  at infinity. So we can introduce  $\mathbf{v}^2 = -2\Phi \geq 0$  where  $\mathbf{v}(\mathbf{r}, t)$  is some velocity vector field. Here the value of  $\mathbf{v}^2$  is specified, but not the direction of  $\mathbf{v}$ . Then

$$\mathbf{g} = \frac{1}{2}\nabla(\mathbf{v}^2) = (\mathbf{v} \cdot \nabla)\mathbf{v} + \mathbf{v} \times (\nabla \times \mathbf{v}). \quad (3)$$

For irrotational flow  $\nabla \times \mathbf{v} = \mathbf{0}$ . Then  $\mathbf{g}$  is the usual Euler expression for the acceleration of a fluid element in a time-independent or stationary fluid flow. If the flow is time dependent and irrotational that expression is expected to become

$$\mathbf{g} = (\mathbf{v} \cdot \nabla)\mathbf{v} + \frac{\partial \mathbf{v}}{\partial t}. \quad (4)$$

Then to be consistent with (1) in the case of a time-dependent matter density the ‘fluid flow’ form of Newtonian gravity is

$$\frac{\partial}{\partial t}(\nabla \cdot \mathbf{v}) + \frac{1}{2}\nabla^2(\mathbf{v}^2) = -4\pi G\rho. \quad (5)$$

This ‘fluid flow’ system has wave-like solutions, in general, but these waves do not manifest as a force via  $\mathbf{g}$ . But, as we shall see later, the flow velocity field  $\mathbf{v}$  is observable, and the experimental data reveals not only  $\mathbf{v}$  but this wave phenomenon. In the generalisation of (5), namely (47), the wave phenomenon does affect  $\mathbf{g}$ . There is experimental evidence that this effect has also been observed, as discussed in sect.2.10. Of course within the fluid flow interpretation (4) and (5) are together equivalent to the Universal Inverse Square Law for Gravity. Indeed for a spherically symmetric distribution of matter of total mass  $M$  the stationary velocity field outside of the matter

$$\mathbf{v}(\mathbf{r}) = -\sqrt{\frac{2GM}{r}}\hat{\mathbf{r}}, \quad (6)$$

satisfies (5) and reproduces the inverse square law form for  $\mathbf{g}$  using (4):

$$\mathbf{g} = -\frac{GM}{r^2}\hat{\mathbf{r}}. \quad (7)$$

The in-flow direction  $-\hat{\mathbf{r}}$  in (6) may be replaced by any other direction, in which case however the direction of  $\mathbf{g}$  in (7) remains radial.

As we shall see of the many new effects predicted by the generalisation of (5) one is that this ‘Inverse Square Law’ is only valid outside of spherically symmetric matter systems. Then, for example, the ‘Inverse Square Law’ is expected to be inapplicable to spiral galaxies. The incorrect assumption of the universal validity of this law led to the notion of ‘dark matter’ in order to reconcile the faster observed rotation velocities of matter within such galaxies compared to that predicted by the above law.

To arrive at the new in-flow theory of gravity we require that the velocity field  $\mathbf{v}(\mathbf{r}, t)$  be specified and measurable with respect to a suitable frame of reference. We shall use the Cosmic Microwave Background (CMB) frame of reference for that purpose [22]. Then a ‘test object’ has velocity  $\mathbf{v}_0(t) = d\mathbf{r}_0(t)/dt$  with respect to that CMB frame, where  $\mathbf{r}_0(t)$  is the position of the object wrt that frame. We then define

$$\mathbf{v}_R(t) = \mathbf{v}_0(t) - \mathbf{v}(\mathbf{r}_0(t), t), \quad (8)$$

as the velocity of the test object relative to the quantum foam at the location of the object.

Process Physics [1] leads to the Lorentzian interpretation of so called ‘relativistic effects’. This means that the speed of light is only ‘c’ with respect to the quantum-foam system, and that time dilation effects for clocks and length contraction effects for rods are caused by the motion of clocks and rods relative

to the quantum foam. So these effects are real dynamical effects caused by the quantum foam, and are not to be interpreted as spacetime effects as suggested by Einstein. To arrive at the dynamical description of the various effects of the quantum foam we shall introduce conjectures that essentially lead to a phenomenological description of these effects. In the future we expect to be able to derive this dynamics directly from the Quantum Homotopic Field Theory formalism [2] that emerges from the information-theoretic system.

First we shall conjecture that the path of an object through an inhomogeneous and time-varying quantum-foam is determined by a variational principle, namely the path  $\mathbf{r}_0(t)$  minimises the travel time

$$\tau[\mathbf{r}_0] = \int dt \left(1 - \frac{\mathbf{v}_R^2}{c^2}\right)^{1/2}, \quad (9)$$

with  $\mathbf{v}_R$  given by (8). Under a deformation of the trajectory  $\mathbf{r}_0(t) \rightarrow \mathbf{r}_0(t) + \delta\mathbf{r}_0(t)$ ,  $\mathbf{v}_0(t) \rightarrow \mathbf{v}_0(t) + \frac{d\delta\mathbf{r}_0(t)}{dt}$ , and we also have

$$\mathbf{v}(\mathbf{r}_0(t) + \delta\mathbf{r}_0(t), t) = \mathbf{v}(\mathbf{r}_0(t), t) + (\delta\mathbf{r}_0(t) \cdot \nabla) \mathbf{v}(\mathbf{r}_0(t)) + \dots \quad (10)$$

Then

$$\begin{aligned} \delta\tau &= \tau[\mathbf{r}_0 + \delta\mathbf{r}_0] - \tau[\mathbf{r}_0] \\ &= - \int dt \frac{1}{c^2} \mathbf{v}_R \cdot \delta\mathbf{v}_R \left(1 - \frac{\mathbf{v}_R^2}{c^2}\right)^{-1/2} + \dots \\ &= \int dt \frac{1}{c^2} \left( \mathbf{v}_R \cdot (\delta\mathbf{r}_0 \cdot \nabla) \mathbf{v} - \mathbf{v}_R \cdot \frac{d(\delta\mathbf{r}_0)}{dt} \right) \left(1 - \frac{\mathbf{v}_R^2}{c^2}\right)^{-1/2} + \dots \\ &= \int dt \frac{1}{c^2} \left( \frac{\mathbf{v}_R \cdot (\delta\mathbf{r}_0 \cdot \nabla) \mathbf{v}}{\sqrt{1 - \frac{\mathbf{v}_R^2}{c^2}}} + \delta\mathbf{r}_0 \cdot \frac{d}{dt} \frac{\mathbf{v}_R}{\sqrt{1 - \frac{\mathbf{v}_R^2}{c^2}}} \right) + \dots \\ &= \int dt \frac{1}{c^2} \delta\mathbf{r}_0 \cdot \left( \frac{(\mathbf{v}_R \cdot \nabla) \mathbf{v} + \mathbf{v}_R \times (\nabla \times \mathbf{v})}{\sqrt{1 - \frac{\mathbf{v}_R^2}{c^2}}} + \frac{d}{dt} \frac{\mathbf{v}_R}{\sqrt{1 - \frac{\mathbf{v}_R^2}{c^2}}} \right) + \dots \end{aligned} \quad (11)$$

Hence a trajectory  $\mathbf{r}_0(t)$  determined by  $\delta\tau = 0$  to  $O(\delta\mathbf{r}_0(t)^2)$  satisfies

$$\frac{d}{dt} \frac{\mathbf{v}_R}{\sqrt{1 - \frac{\mathbf{v}_R^2}{c^2}}} = - \frac{(\mathbf{v}_R \cdot \nabla) \mathbf{v} + \mathbf{v}_R \times (\nabla \times \mathbf{v})}{\sqrt{1 - \frac{\mathbf{v}_R^2}{c^2}}}. \quad (12)$$

Let us now write this in a more explicit form. This will also allow the low speed limit to be identified. Substituting  $\mathbf{v}_R(t) = \mathbf{v}_0(t) - \mathbf{v}(\mathbf{r}_0(t), t)$  and using

$$\frac{d\mathbf{v}(\mathbf{r}_0(t), t)}{dt} = (\mathbf{v}_0 \cdot \nabla) \mathbf{v} + \frac{\partial \mathbf{v}}{\partial t}, \quad (13)$$

we obtain

$$\frac{d}{dt} \frac{\mathbf{v}_0}{\sqrt{1 - \frac{\mathbf{v}_R^2}{c^2}}} = \mathbf{v} \frac{d}{dt} \frac{1}{\sqrt{1 - \frac{\mathbf{v}_R^2}{c^2}}} + \frac{(\mathbf{v} \cdot \nabla) \mathbf{v} - \mathbf{v}_R \times (\nabla \times \mathbf{v}) + \frac{\partial \mathbf{v}}{\partial t}}{\sqrt{1 - \frac{\mathbf{v}_R^2}{c^2}}}. \quad (14)$$

Then in the low speed limit  $v_R \ll c$  we obtain

$$\frac{d\mathbf{v}_0}{dt} = (\mathbf{v} \cdot \nabla) \mathbf{v} - \mathbf{v}_R \times (\nabla \times \mathbf{v}) + \frac{\partial \mathbf{v}}{\partial t} = \mathbf{g}(\mathbf{r}_0(t), t) + (\nabla \times \mathbf{v}) \times \mathbf{v}_0, \quad (15)$$

which agrees with the ‘Newtonian’ form (4) for zero vorticity ( $\nabla \times \mathbf{v} = 0$ ). Hence (14) is a generalisation of (4) to include Lorentzian dynamical effects, for in (14) we can multiply both sides by the rest mass  $m_0$  of the object, and then (14) involves

$$m(\mathbf{v}_R) = \frac{m_0}{\sqrt{1 - \frac{\mathbf{v}_R^2}{c^2}}}, \quad (16)$$

the so called ‘relativistic’ mass, and (14) acquires the form

$$\frac{d}{dt} (m(\mathbf{v}_R) \mathbf{v}_0) = \mathbf{F},$$

where  $\mathbf{F}$  is an effective ‘force’ caused by the inhomogeneities and time-variation of the flow. This is essentially Newton’s 2nd Law of Motion in the case of gravity only. That  $m_0$  cancels is the equivalence principle, and which acquires a simple explanation in terms of the flow. Note that the occurrence of  $1/\sqrt{1 - \frac{\mathbf{v}_R^2}{c^2}}$  will lead to the precession of the perihelion of planetary orbits, and also to horizon effects wherever  $|\mathbf{v}| = c$ : the region where  $|\mathbf{v}| < c$  is inaccessible from the region where  $|\mathbf{v}| > c$ .

Eqn.(9) involves various absolute quantities such as the absolute velocity of an object relative to the quantum foam and the absolute speed  $c$  also relative to the foam, and of course absolute velocities are excluded from the General Relativity (GR) formalism. However (9) gives (with  $t = x_0^0$ )

$$d\tau^2 = dt^2 - \frac{1}{c^2} (d\mathbf{r}_0(t) - \mathbf{v}(\mathbf{r}_0(t), t) dt)^2 = g_{\mu\nu}(x_0) dx_0^\mu dx_0^\nu, \quad (17)$$

which is the Panlevé-Gullstrand form of the metric  $g_{\mu\nu}$  [23, 24] for GR. All of the above is very suggestive that useful information for the flow dynamics may be obtained from GR by restricting the choice of metric to the Panlevé-Gullstrand form. We emphasize that the absolute velocity  $\mathbf{v}_R$  has been measured, and so the foundations of GR as usually stated are invalid. As we shall now see the GR formalism involves two phenomena, namely (i) the use of an unnecessarily restrictive Einstein measurement protocol and (ii) the Lorentzian quantum-foam dynamical effects. Later we shall remove this measurement protocol from GR and discover that the GR formalism reduces to explicit fluid flow equations. However to understand the GR formalism we need to explicitly introduce the troublesome Einstein measurement protocol and the peculiar effects that it induces in the observers historical records.

## 2.2 The Einstein Measurement Protocol

The quantum foam, it is argued, induces actual dynamical time dilations and length contractions in agreement with the Lorentz interpretation of special relativistic effects. Then observers in uniform motion ‘through’ the foam will on measurement of the speed of light obtain always the same numerical value  $c$ . To see this explicitly consider how various observers  $P, P', ..$  moving with different speeds through the foam, measure the speed of light. They each acquire a standard rod and an accompanying standardised clock. That means that these standard rods would agree if they were brought together, and at rest with respect to the quantum foam they would all have length  $\Delta l_0$ , and similarly for the clocks. Observer  $P$  and accompanying rod are both moving at speed  $v_R$  relative to the quantum foam, with the rod longitudinal to that motion.  $P$  then measures the time  $\Delta t_R$ , with the clock at end  $A$  of the rod, for a light pulse to travel from end  $A$  to the other end  $B$  and back again to  $A$ . The light travels at speed  $c$  relative to the quantum-foam. Let the time taken for the light pulse to travel from  $A \rightarrow B$  be  $t_{AB}$  and from  $B \rightarrow A$  be  $t_{BA}$ , as measured by a clock at rest with respect to the quantum foam<sup>1</sup>. The length of the rod moving at speed  $v_R$  is contracted to

$$\Delta l_R = \Delta l_0 \sqrt{1 - \frac{v_R^2}{c^2}}. \quad (18)$$

In moving from  $A$  to  $B$  the light must travel an extra distance because the end  $B$  travels a distance  $v_R t_{AB}$  in this time, thus the total distance that must be traversed is

$$ct_{AB} = \Delta l_R + v_R t_{AB}, \quad (19)$$

Similarly on returning from  $B$  to  $A$  the light must travel the distance

$$ct_{BA} = \Delta l_R - v_R t_{BA}. \quad (20)$$

Hence the total travel time  $\Delta t_0$  is

$$\Delta t_0 = t_{AB} + t_{BA} = \frac{\Delta l_R}{c - v_R} + \frac{\Delta l_R}{c + v_R} \quad (21)$$

$$= \frac{2\Delta l_0}{c\sqrt{1 - \frac{v_R^2}{c^2}}}. \quad (22)$$

Because of the time dilation effect for the moving clock

$$\Delta t_R = \Delta t_0 \sqrt{1 - \frac{v_R^2}{c^2}}. \quad (23)$$

Then for the moving observer the speed of light is defined as the distance the observer believes the light travelled ( $2\Delta l_0$ ) divided by the travel time according to the accompanying clock ( $\Delta t_R$ ), namely  $2\Delta l_0/\Delta t_R = c$ . So the speed  $v_R$  of the

<sup>1</sup>Not all clocks will behave in this same ‘ideal’ manner.



observer through the quantum foam is not revealed by this procedure, and the observer is erroneously led to the conclusion that the speed of light is always  $c$ . This follows from two or more observers in manifest relative motion all obtaining the same speed  $c$  by this procedure. Despite this failure this special effect is actually the basis of the spacetime Einstein measurement protocol. That this protocol is blind to the absolute motion has led to enormous confusion within physics.

To be explicit the Einstein measurement protocol actually inadvertently uses this special effect by using the radar method for assigning historical spacetime coordinates to an event: the observer records the time of emission and reception of radar pulses ( $t_r > t_e$ ) travelling through the space of quantum foam, and then retrospectively assigns the time and distance of a distant event  $B$  according to (ignoring directional information for simplicity)

$$T_B = \frac{1}{2}(t_r + t_e), \quad D_B = \frac{c}{2}(t_r - t_e), \quad (24)$$

where each observer is now using the same numerical value of  $c$ . The event  $B$  is then plotted as a point in an individual geometrical construct by each observer, known as a spacetime record, with coordinates  $(D_B, T_B)$ . This is no different to an historian recording events according to some agreed protocol. Unlike historians, who don't confuse history books with reality, physicists do so. We now show that because of this protocol and the quantum foam dynamical effects, observers will discover on comparing their historical records of the same events that the expression

$$\tau_{AB}^2 = T_{AB}^2 - \frac{1}{c^2}D_{AB}^2, \quad (25)$$

is an invariant, where  $T_{AB} = T_A - T_B$  and  $D_{AB} = D_A - D_B$  are the differences in times and distances assigned to events  $A$  and  $B$  using the Einstein measurement protocol (24), so long as both are sufficiently small compared with the scale of inhomogeneities in the velocity field.

To confirm the invariant nature of the construct in (25) one must pay careful attention to observational times as distinct from protocol times and distances, and this must be done separately for each observer. This can be tedious. We now demonstrate this for the situation illustrated in Fig.1.

By definition the speed of  $P'$  according to  $P$  is  $v'_0 = D_B/T_B$  and so  $v'_R = v'_0$ , where  $T_B$  and  $D_B$  are the protocol time and distance for event  $B$  for observer  $P$  according to (24). Then using (25)  $P$  would find that  $(\tau_{AB}^P)^2 = T_B^2 - \frac{1}{c^2}D_B^2$  since both  $T_A = 0$  and  $D_A = 0$ , and whence  $(\tau_{AB}^P)^2 = (1 - \frac{v'^2_0}{c^2})T_B^2 = (t'_B)^2$  where the last equality follows from the time dilation effect on the  $P'$  clock, since  $t'_B$  is the time of event  $B$  according to that clock. Then  $T_B$  is also the time that  $P'$  would compute for event  $B$  when correcting for the time-dilation effect, as the speed  $v'_R$  of  $P'$  through the quantum foam is observable by  $P'$ . Then  $T_B$  is the 'common time' for event  $B$  assigned by both observers<sup>2</sup>. For  $P'$  we obtain

<sup>2</sup>Because of gravitational in-flow effects this 'common time' is not the same as a 'universal' or 'absolute time'; see later.

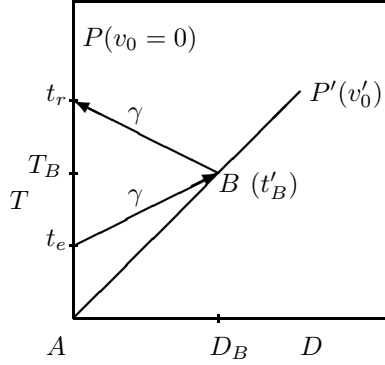


Figure 1: Here  $T - D$  is the spacetime construct (from the Einstein measurement protocol) of a special observer  $P$  at rest wrt the quantum foam, so that  $v_0 = 0$ . Observer  $P'$  is moving with speed  $v'_0$  as determined by observer  $P$ , and therefore with speed  $v'_R = v'_0$  wrt the quantum foam. Two light pulses are shown, each travelling at speed  $c$  wrt both  $P$  and the quantum foam. As we see later these one-way speeds for light, relative to the quantum foam, are equal by observation. Event  $A$  is when the observers pass, and is also used to define zero time for each for convenience.

directly, also from (24) and (25), that  $(\tau_{AB}^{P'})^2 = (T'_B)^2 - \frac{1}{c^2}(D'_B)^2 = (t'_B)^2$ , as  $D'_B = 0$  and  $T'_B = t'_B$ . Whence for this situation

$$(\tau_{AB}^P)^2 = (\tau_{AB}^{P'})^2, \quad (26)$$

and so the construction (25) is an invariant.

While so far we have only established the invariance of the construct (25) when one of the observers is at rest wrt to the quantum foam, it follows that for two observers  $P'$  and  $P''$  both in motion wrt the quantum foam it follows that they also agree on the invariance of (25). This is easily seen by using the intermediate step of a stationary observer  $P$ :

$$(\tau_{AB}^{P'})^2 = (\tau_{AB}^P)^2 = (\tau_{AB}^{P''})^2. \quad (27)$$

Hence the protocol and Lorentzian effects result in the construction in (25) being indeed an invariant in general. This is a remarkable and subtle result. For Einstein this invariance was a fundamental assumption, but here it is a derived result, but one which is nevertheless deeply misleading. Explicitly indicating small quantities by  $\Delta$  prefixes, and on comparing records retrospectively, an ensemble of nearby observers agree on the invariant

$$\Delta\tau^2 = \Delta T^2 - \frac{1}{c^2}\Delta D^2, \quad (28)$$

for any two nearby events. This implies that their individual patches of spacetime records may be mapped one into the other merely by a change of coordinates, and that collectively the spacetime patches of all may be represented

by one pseudo-Riemannian manifold, where the choice of coordinates for this manifold is arbitrary, and we finally arrive at the invariant

$$\Delta\tau^2 = \eta_{\mu\nu}(x)\Delta x^\mu \Delta x^\nu, \quad (29)$$

with  $x^\mu = \{T, D_1, D_2, D_3\}$  and  $\eta_{\mu\nu}$  the usual metric of the spacetime construct. Eqn.(29) is of course invariant under the Lorentz transformation.

### 2.3 The Origins of General Relativity

Above it was seen that the Lorentz symmetry of the spacetime construct would arise if the quantum foam system that forms space affects the rods and clocks used by observers in the manner indicated. The effects of absolute motion with respect to this quantum foam are in fact easily observed, and so the velocity  $\mathbf{v}_R$  of each observer is measurable. However if we work only with the spacetime construct then the effects of the absolute motion are hidden. Einstein was very much misled by the reporting of the experiment by Michelson and Morley of 1887, as now it is apparent that this experiment, and others since then, revealed evidence of absolute motion. The misunderstanding of the Michelson-Morley experiment had a major effect on the subsequent development of physics. One such development was the work of Hilbert and Einstein in finding an apparent generalisation of Newtonian gravity to take into account the apparent absence of absolute motion. Despite the deep error in this work the final formulation, known as General Relativity, has had a number of successes including the perihelion precession of mercury, the bending of light and gravitational red shift. Hence despite the incorrect treatment of absolute motion the formalism of general relativity apparently has some validity. In the next section we shall *deconstruct* this formalism to discover its underlying physics, but here we first briefly outline the GR formalism.

The spacetime construct is a static geometrical non-processing historical record, and is nothing more than a very refined history book, with the shape of the manifold encoded in a metric tensor  $g_{\mu\nu}(x)$ . However in a formal treatment by Einstein the SR formalism and later the GR formalism is seen to arise from three fundamental assumptions:

- (1) **The laws of physics have the same form in all inertial reference frames.**
  - (2) **Light propagates through empty space with a definite speed  $c$  independent of the speed of the source or observer.**
  - (3) **In the limit of low speeds the new formalism should agree with Newtonian gravity.**
- (30)

There is strong experimental evidence that all three of these assumptions are in fact wrong (except for the 2nd part of (2)). Nevertheless there is something that is partially correct within the formalism, and that part needs to

be extracted and saved, with the rest discarded. From the above assumptions Hilbert and Einstein guessed the equation which specifies the metric tensor  $g_{\mu\nu}(x)$ , namely the geometry of the spacetime construct,

$$G_{\mu\nu} \equiv R_{\mu\nu} - \frac{1}{2}Rg_{\mu\nu} = \frac{8\pi G}{c^2}T_{\mu\nu}, \quad (31)$$

where  $G_{\mu\nu}$  is known as the Einstein tensor,  $T_{\mu\nu}$  is the energy-momentum tensor,  $R_{\mu\nu} = R_{\mu\alpha\nu}^{\alpha}$  and  $R = g^{\mu\nu}R_{\mu\nu}$  and  $g^{\mu\nu}$  is the matrix inverse of  $g_{\mu\nu}$ . The curvature tensor is

$$R_{\mu\sigma\nu}^{\rho} = \Gamma_{\mu\nu,\sigma}^{\rho} - \Gamma_{\mu\sigma,\nu}^{\rho} + \Gamma_{\alpha\sigma}^{\rho}\Gamma_{\mu\nu}^{\alpha} - \Gamma_{\alpha\nu}^{\rho}\Gamma_{\mu\sigma}^{\alpha}, \quad (32)$$

where  $\Gamma_{\mu\sigma}^{\alpha}$  is the affine connection

$$\Gamma_{\mu\sigma}^{\alpha} = \frac{1}{2}g^{\alpha\nu} \left( \frac{\partial g_{\nu\mu}}{\partial x^{\sigma}} + \frac{\partial g_{\nu\sigma}}{\partial x^{\mu}} - \frac{\partial g_{\mu\sigma}}{\partial x^{\nu}} \right). \quad (33)$$

In this formalism the trajectories of test objects are determined by

$$\Gamma_{\mu\nu}^{\lambda} \frac{dx^{\mu}}{d\tau} \frac{dx^{\nu}}{d\tau} + \frac{d^2x^{\lambda}}{d\tau^2} = 0, \quad (34)$$

which is equivalent to minimising the functional

$$\tau[x] = \int dt \sqrt{g^{\mu\nu} \frac{dx^{\mu}}{dt} \frac{dx^{\nu}}{dt}}, \quad (35)$$

wrt to the path  $x[t]$ .

For the case of a spherically symmetric mass a solution of (31) for  $g_{\mu\nu}$  outside of that mass  $M$  is the Schwarzschild metric

$$d\tau^2 = \left(1 - \frac{2GM}{c^2 r}\right) dt^2 - \frac{1}{c^2} r^2 (d\theta^2 + \sin^2(\theta) d\phi^2) - \frac{dr^2}{c^2 \left(1 - \frac{2GM}{c^2 r}\right)}. \quad (36)$$

This solution is the basis of various experimental checks of General Relativity in which the spherically symmetric mass is either the sun or the earth. The four tests are: the gravitational redshift, the bending of light, the precession of the perihelion of mercury, and the time delay of radar signals.

However the solution (36) is in fact completely equivalent to the in-flow interpretation of Newtonian gravity. Making the change of variables  $t \rightarrow t'$  and  $\mathbf{r} \rightarrow \mathbf{r}' = \mathbf{r}$  with

$$t' = t + \frac{2}{c} \sqrt{\frac{2GM}{c^2} r} - \frac{4GM}{c^2} \tanh^{-1} \sqrt{\frac{2GM}{c^2 r}}, \quad (37)$$

the Schwarzschild solution (36) takes the form

$$d\tau^2 = dt'^2 - \frac{1}{c^2} (dr' + \sqrt{\frac{2GM}{r'}} dt')^2 - \frac{1}{c^2} r'^2 (d\theta'^2 + \sin^2(\theta') d\phi'^2), \quad (38)$$

which is exactly the Panlevé-Gullstrand form of the metric  $g_{\mu\nu}$  [23, 24] in (17) with the velocity field given exactly by the Newtonian form in (6). In which case the trajectory equation (34) of test objects in the Schwarzschild metric is equivalent to solving (14). Thus the minimisation (35) is equivalent to that of (9). This choice of coordinates corresponds to a particular frame of reference in which the test object has velocity  $\mathbf{v}_R = \mathbf{v} - \mathbf{v}_0$  relative to the in-flow field  $\mathbf{v}$ , as seen in (9).

It is conventional wisdom for practitioners in General Relativity to regard the choice of coordinates or frame of reference to be entirely arbitrary and having no physical significance: no observations should be possible that can detect and measure  $\mathbf{v}_R$ . This ‘wisdom’ is based on two beliefs (i) that all attempts to detect  $\mathbf{v}_R$ , namely the detection of absolute motion, have failed, and that (ii) the existence of absolute motion is incompatible with the many successes of both the Special Theory of Relativity and of the General Theory of Relativity. Both of these beliefs are demonstrably false.

The results in this section suggest, just as for Newtonian gravity, that the Einstein General Relativity is nothing more than the dynamical equations for a velocity flow field  $\mathbf{v}(\mathbf{r}, t)$ . Hence the spacetime construct appears to be merely an unnecessary artifact of the Einstein measurement protocol, which in turn was motivated by the mis-reporting of the results of the Michelson-Morley experiment. The successes of General Relativity should thus be considered as an insight into the fluid flow dynamics of the quantum foam system, rather than any confirmation of the validity of the spacetime formalism. In the next section we shall deconstruct General Relativity to extract a possible form for this dynamics.

## 2.4 Deconstruction of General Relativity

Here we deconstruct the formalism of General Relativity by removing the obscurification produced by the unnecessarily restricted Einstein measurement protocol. To do this we adopt the Panlevé-Gullstrand form of the metric  $g_{\mu\nu}$  as that corresponding to the observable quantum foam system, namely to an observationally detected special frame of reference. This form for the metric involves a general velocity field  $\mathbf{v}(\mathbf{r}, t)$  where for precision we consider the coordinates  $\mathbf{r}, t$  as that of observers at rest with respect to the CMB frame. Note that in this frame  $\mathbf{v}(\mathbf{r}, t)$  is not necessarily zero, for mass acts as a sink for the flow. We therefore merely substitute the metric

$$d\tau^2 = g_{\mu\nu} dx^\mu dx^\nu = dt^2 - \frac{1}{c^2} (d\mathbf{r}(t) - \mathbf{v}(\mathbf{r}(t), t) dt)^2, \quad (39)$$

into (31) using (33) and (32). This metric involves the arbitrary time-dependent velocity field  $\mathbf{v}(\mathbf{r}, t)$ . This is a very tedious computation and the results below were obtained by using the symbolic mathematics capabilities of *Mathematica*.

The various components of the Einstein tensor are then

$$\begin{aligned}
G_{00} &= \sum_{i,j=1,2,3} v_i \mathcal{G}_{ij} v_j - c^2 \sum_{j=1,2,3} \mathcal{G}_{0j} v_j - c^2 \sum_{i=1,2,3} v_i \mathcal{G}_{i0} + c^2 \mathcal{G}_{00}, \\
G_{i0} &= - \sum_{j=1,2,3} \mathcal{G}_{ij} v_j + c^2 \mathcal{G}_{i0}, \quad i = 1, 2, 3. \\
G_{ij} &= \mathcal{G}_{ij}, \quad i, j = 1, 2, 3.
\end{aligned} \tag{40}$$

where the  $\mathcal{G}_{\mu\nu}$  are given by

$$\begin{aligned}
\mathcal{G}_{00} &= \frac{1}{2}((trD)^2 - tr(D^2)), \\
\mathcal{G}_{i0} &= \mathcal{G}_{0i} = -\frac{1}{2}(\nabla \times (\nabla \times \mathbf{v}))_i, \quad i = 1, 2, 3. \\
\mathcal{G}_{ij} &= \frac{d}{dt}(D_{ij} - \delta_{ij} trD) + (D_{ij} - \frac{1}{2} \delta_{ij} trD) trD \\
&\quad - \frac{1}{2} \delta_{ij} tr(D^2) - (D\Omega - \Omega D)_{ij}, \quad i, j = 1, 2, 3.
\end{aligned} \tag{41}$$

Here

$$D_{ij} = \frac{1}{2} \left( \frac{\partial v_i}{\partial x_j} + \frac{\partial v_j}{\partial x_i} \right) \tag{42}$$

is the symmetric part of the rate of strain tensor  $\frac{\partial v_i}{\partial x_j}$ , while the antisymmetric part is

$$\Omega_{ij} = \frac{1}{2} \left( \frac{\partial v_i}{\partial x_j} - \frac{\partial v_j}{\partial x_i} \right). \tag{43}$$

In vacuum, with  $T_{\mu\nu} = 0$ , we find from (31) and (40) that  $G_{\mu\nu} = 0$  implies that  $\mathcal{G}_{\mu\nu} = 0$ . It is then easy to check that the in-flow velocity field (6) satisfies these equations. This simply expresses the previous observation that this ‘Newtonian in-flow’ is completely equivalent to the Schwarzschild metric. We note that the vacuum equations  $\mathcal{G}_{\mu\nu} = 0$  do not involve the speed of light; it appears only in (40). It is therefore suggested that (40) amounts to the separation of the Einstein measurement protocol, which involves  $c$ , from the supposed dynamics of gravity within the GR formalism, and which does not involve  $c$ . However the details of the vacuum dynamics in (41) have not actually been tested. All the key tests of GR are now seen to amount to a test *only* of  $\delta\tau[x]/\delta x^\mu = 0$ , which is the minimisation of (9), when the in-flow field is given by (40), and which is nothing more than Newtonian gravity. Of course Newtonian gravity was itself merely based upon observations within the solar system, and this may have been too special to have revealed key aspects of gravity. Hence, despite popular opinion, the GR formalism is apparently based upon rather poor evidence.

## 2.5 The New Theory of Gravity

Despite the limited insight into gravity which GR is now seen to amount to, here we look for possible generalisations of Newtonian gravity and its in-flow

interpretation by examining some of the mathematical structures that have arisen in (41). For the case of zero vorticity  $\nabla \times \mathbf{v} = 0$  we have  $\Omega_{ij} = 0$  and also that we may write  $\mathbf{v} = \nabla u$  where  $u(\mathbf{r}, t)$  is a scalar field, and only one equation is required to determine  $u$ . To that end we consider the trace of  $\mathcal{G}_{ij}$ . Note that  $tr(D) = \nabla \cdot \mathbf{v}$ , and that

$$\frac{d(\nabla \cdot \mathbf{v})}{dt} = (\mathbf{v} \cdot \nabla)(\nabla \cdot \mathbf{v}) + \frac{\partial(\nabla \cdot \mathbf{v})}{\partial t}. \quad (44)$$

Then using the identity

$$(\mathbf{v} \cdot \nabla)(\nabla \cdot \mathbf{v}) = \frac{1}{2} \nabla^2(\mathbf{v}^2) - tr(D^2) - \frac{1}{2}(\nabla \times \mathbf{v})^2 + \mathbf{v} \cdot \nabla \times (\nabla \times \mathbf{v}), \quad (45)$$

and imposing

$$\sum_{i=1,2,3} \mathcal{G}_{ii} = -8\pi G\rho, \quad (46)$$

we obtain

$$\frac{\partial}{\partial t}(\nabla \cdot \mathbf{v}) + \frac{1}{2} \nabla^2(\mathbf{v}^2) + \frac{\delta}{4}((trD)^2 - tr(D^2)) = -4\pi G\rho. \quad (47)$$

with  $\delta = 1$ . However GR via (41) also stipulates that  $\frac{1}{4}((trD)^2 - tr(D^2)) = 0$  in vacuum, implying that overall  $\delta = 0$  in GR. So (47) with  $\delta \neq 0$  is not equivalent to GR. Nevertheless this is seen to be a possible generalisation of the Newtonian equation (5) that includes the new term  $C(\mathbf{v}) = \frac{\delta}{4}((trD)^2 - tr(D^2))$ . It appears that the existence and significance of this new term has gone unnoticed for some 300 years. Its presence explains the many known gravitational anomalies, as we shall see. Eqn.(47) describes the flow of space and its self-interaction. The value of  $\delta$  should be determined from both the underlying theory and also by analysis of experimental data; see Sects.2.9 and 2.11. We also note that because of the  $C(\mathbf{v})$  term  $G$  does not necessarily have the same value as the value  $G_N$  determined by say Cavendish type experiments.

The most significant aspect of (47) is that the new term  $C(\mathbf{v}) = 0$  only for the in-flow velocity field in (6), namely only outside of a spherically symmetric matter distribution.

Hence (47) in the case of the solar system is indistinguishable from Newtonian gravity, or the Schwarzschild metric within the General Relativity formalism so long as we use (9), in being able to determine trajectories of test objects. Hence (47) is automatically in agreement with most of the so-called checks on Newtonian gravity and later General Relativity. Note that (47) does not involve the speed of light  $c$ . Nevertheless we have not derived (47) from the underlying Quantum Homotopic Field Theory, and indeed it is not a consequence of GR, as the  $\mathcal{G}_{00}$  equation of (41) requires that  $C(\mathbf{v}) = 0$  in vacuum. Eqn.(47) at this stage should be regarded as a conjecture which will permit the exploration of possible quantum-flow physics and also allow comparison with experiment.

However one key aspect of (47) should be noted here, namely that being a non-linear fluid-flow dynamical system we would expect the flow to be turbulent, particularly when the matter is not spherically symmetric or inside even

a spherically symmetric distribution of matter, since then the  $C(\mathbf{v})$  term is non-zero and it will drive that turbulence. We see that the experiments that reveal absolute motion also reveal evidence of such turbulence - a new form of gravitational wave predicted by the new theory of gravity.

## 2.6 The ‘Dark Matter’ Effect

Because of the  $C(\mathbf{v})$  term (47) would predict that the Newtonian inverse square law would not be applicable to systems such as spiral galaxies, because of their highly non-spherical distribution of matter. Of course attempts to retain this law, despite its manifest failure, has led to the spurious introduction of the notion of dark matter within spiral galaxies, and also at larger scales. From

$$\mathbf{g} = \frac{1}{2}\nabla(\mathbf{v}^2) + \frac{\partial\mathbf{v}}{\partial t}, \quad (48)$$

which is (4) for irrotational flow, we see that (47) gives

$$\nabla\cdot\mathbf{g} = -4\pi G\rho - C(\mathbf{v}), \quad (49)$$

and taking running time averages to account for turbulence

$$\nabla\cdot\langle\mathbf{g}\rangle = -4\pi G\rho - \langle C(\mathbf{v})\rangle, \quad (50)$$

and writing the extra term as  $\langle C(\mathbf{v})\rangle = 4\pi G\rho_{DM}$  we see that  $\rho_{DM}$  would act as an effective matter density, and it is suggested that it is the consequences of this term which have been misinterpreted as ‘dark matter’. Here we see that this effect is actually the consequence of quantum foam effects within the new proposed dynamics for gravity, and which becomes apparent particularly in spiral galaxies. Because  $\nabla \times \mathbf{v} = 0$  we can write (47) in the form

$$\mathbf{v}(\mathbf{r}, t) =$$

$$\int^t dt' \int d^3r' (\mathbf{r} - \mathbf{r}') \frac{\frac{1}{2}\nabla^2(\mathbf{v}^2(\mathbf{r}', t')) + 4\pi G\rho(\mathbf{r}', t') + C(\mathbf{v}(\mathbf{r}', t'))}{4\pi|\mathbf{r} - \mathbf{r}'|^3}, \quad (51)$$

which allows the determination of the time evolution of  $\mathbf{v}$ .

In practice it is easier to compute the vortex-free velocity field from a velocity potential according to  $\mathbf{v}(\mathbf{r}, t) = \nabla u(\mathbf{r}, t)$ , and we find the integro-differential equation for  $u(\mathbf{r}, t)$

$$\frac{\partial u(\mathbf{r}, t)}{\partial t} = -\frac{1}{2}(\nabla u(\mathbf{r}, t))^2 + \frac{1}{4\pi} \int d^3r' \frac{C(\nabla u(\mathbf{r}', t))}{|\mathbf{r} - \mathbf{r}'|} - \Phi(\mathbf{r}, t), \quad (52)$$

where  $\Phi$  is the Newtonian gravitational potential

$$\Phi(\mathbf{r}, t) = -G \int d^3r' \frac{\rho(\mathbf{r}', t)}{|\mathbf{r} - \mathbf{r}'|}. \quad (53)$$



Hence the  $\Phi$  field acts as the source term for the velocity potential. Note that in the Newtonian theory of gravity one has the choice of using either the acceleration field  $\mathbf{g}$  or the velocity field  $\mathbf{v}$ . However in the new theory of gravity this choice is no longer available: the fundamental dynamical degree of freedom is necessarily the  $\mathbf{v}$  field, again because of the presence of the  $C(\mathbf{v})$  term, which obviously cannot be written in terms of  $\mathbf{g}$ .

The new flow dynamics encompassed in (47) thus accounts for most of the known gravitational phenomena, but will lead to some very clear cut experiments that will distinguish it from the two previous attempts to model gravitation. It turns out that these two attempts were based on some key ‘accidents’ of history. In the case of the Newtonian modelling of gravity the prime ‘accident’ was of course the solar system with its high degree of spherical symmetry. In each case we had test objects, namely the planets, in orbit about the sun, or we had test object in orbit about the earth. In the case of the General Relativity modelling the prime ‘accident’ was the mis-reporting of the Michelson-Morley experiment, and the ongoing belief that the so called ‘relativistic effects’ are incompatible with absolute motion, and of course that GR was constructed to agree with Newtonian gravity in the ‘non-relativistic’ limit, and so ‘inherited’ the flaws of that theory. We shall consider in detail later some further anomalies that might be appropriately explained by this new modelling of gravity. Of course that the in-flow has been present in various experimental data is also a significant argument for something like (47) to model gravity.

## 2.7 In-Flow Superposition Approximation

We consider here why the existence of absolute motion and as well the consequences and so the presence of the  $C(\mathbf{v})$  term appears to have escaped attention in the case of gravitational experiments and observations near the earth, despite the fact, in the case of the  $C(\mathbf{v})$  term, that the presence of the earth breaks the spherical symmetry of the matter distribution of the sun.

First note that if we have a matter distribution  $\rho(\mathbf{r})$  at rest in the space of quantum foam, and that (47) has solution  $\mathbf{v}_0(\mathbf{r}, t)$ , with  $\mathbf{g}_0(\mathbf{r}, t)$  given by (48), then when the same matter distribution is uniformly translating at velocity  $\mathbf{V}$ , that is  $\rho(\mathbf{r}) \rightarrow \rho(\mathbf{r} - \mathbf{V}t)$ , then a solution to (47) is

$$\mathbf{v}(\mathbf{r}, t) = \mathbf{v}_0(\mathbf{r} - \mathbf{V}t, t) + \mathbf{V}. \quad (54)$$

Note that this is a manifestly time-dependent process and the time derivative in (4) or (14) and (47) plays an essential role. As well the result is nontrivial as (47) is a non-linear equation. The solution (54) follows because (i) the expression for the acceleration  $\mathbf{g}(\mathbf{r}, t)$  gives, and this expression occurs in (47),

$$\begin{aligned} \mathbf{g}(\mathbf{r}, t) &= \frac{\partial \mathbf{v}_0(\mathbf{r} - \mathbf{V}t, t)}{\partial t} + ((\mathbf{v}_0(\mathbf{r} - \mathbf{V}t, t) + \mathbf{V}) \cdot \nabla)(\mathbf{v}_0(\mathbf{r} - \mathbf{V}t, t) + \mathbf{V}), \\ &= \frac{\partial \mathbf{v}_0(\mathbf{r} - \mathbf{V}t', t)}{\partial t'} \Big|_{t' \rightarrow t} + \mathbf{g}_0(\mathbf{r} - \mathbf{V}t, t) + (\mathbf{V} \cdot \nabla) \mathbf{v}_0(\mathbf{r} - \mathbf{V}t, t), \end{aligned}$$

$$\begin{aligned}
&= -(\mathbf{V}\cdot\nabla)\mathbf{v}_0(\mathbf{r}-\mathbf{V}t,t) + \mathbf{g}_0(\mathbf{r}-\mathbf{V}t,t) + (\mathbf{V}\cdot\nabla)\mathbf{v}_0(\mathbf{r}-\mathbf{V}t,t), \\
&= \mathbf{g}_0(\mathbf{r}-\mathbf{V}t,t),
\end{aligned} \tag{55}$$

as there is a key cancellation of two terms in (55), and (ii) clearly  $C(\mathbf{v}_0(\mathbf{r}-\mathbf{V}t,t) + \mathbf{V}) = C(\mathbf{v}_0(\mathbf{r}-\mathbf{V}t,t))$ , and so this term is also simply translated. Hence apart from the translation effect the acceleration is the same. Hence the velocity vector addition rule in (54) is valid for generating the vector flow field for the translating matter distribution. This is why the large absolute motion velocity of some 400 km/s of the solar system does not interfere with the usual computation and observation of gravitational forces.

For earth based gravitational phenomena the motion of the earth takes place within the velocity in-flow towards the sun, and the velocity sum rule (54) is only approximately valid as now  $\mathbf{V} \rightarrow \mathbf{V}(\mathbf{r},t)$  and no longer corresponds to uniform translation, and manifests turbulence. To be a valid approximation the inhomogeneity of  $\mathbf{V}(\mathbf{r},t)$  must be much smaller than that of  $\mathbf{v}_0(\mathbf{r}-\mathbf{V}t,t)$ , which it is, as the earth's centripetal acceleration about the sun is approximately 1/1000 that of the earth's gravitational acceleration at the surface of the earth. Nevertheless turbulence associated with the  $C(\mathbf{v})$  term is apparent in experimental data. The validity of this approximation demonstrates that the detection of a cosmic absolute motion and the in-flow theory of gravity are consistent with the older methods of computing gravitational forces. This is why both the presence of the  $C(\mathbf{v})$  term, the in-flow and the absolute motion have gone almost unnoticed in earth based gravitational experiments, except for various anomalies; see section 2.9.

## 2.8 Gravitational In-Flow and the GPS

It has been extensively argued that the very successful operation of the Global Positioning System (GPS) [26] is proof of the validity of the General Relativity formalism for gravity. However as is well known, and was most clearly stated by Popper, in science agreement with observation does not amount to the proof of the theory used to successfully describe the experimental data; in fact experiment can only strictly be used to disprove a theory.

We show here that the new in-flow theory of gravity together with the observed absolute velocity of motion of the solar system through space are together compatible with the operation of the Global Positioning System (GPS). Given the developments above this turns out to be an almost trivial exercise. As usual in this system the effects of the sun and moon are neglected. Various effects need to be included as the system relies upon extremely accurate atomic clocks in the satellites forming the GPS constellation. Within both the new theory and General Relativity these clocks are affected by both their speed and the gravitational effects of the earth. As well the orbits of these satellites and the critical time delays of radio signals from the satellites need to be computed. For the moment we assume spherical symmetry for the earth. The effects of non-sphericity will be discussed below. In General Relativity the orbits and

signalling time delays are determined by the use of the geodesic equation (34) and the Schwarzschild metric (36). However these two equations are equivalent to the orbital equation (16) and the velocity field (54), with a velocity  $\mathbf{V}$  of absolute motion, and with the in-flow given by (6), noting the result in section 2.7. For EM signalling the elapsed time in (9) requires careful treatment. Hence the two systems are completely mathematically equivalent: the computations within the new system may most easily be considered by relating them to the mathematically equivalent General Relativity formalism. We can also see this by explicitly changing from the CMB frame to a non-rotating frame co-moving with the earth by means of the change of variables

$$\begin{aligned} \mathbf{r} &= \mathbf{r}' + \mathbf{V}t', \\ t &= t', \\ \mathbf{v} &= \mathbf{v}' + \mathbf{V}, \end{aligned} \tag{56}$$

which lead to the relationships of differentials

$$\begin{aligned} \nabla' &= \nabla, \\ \frac{\partial}{\partial t'} &= \frac{\partial}{\partial t} + \mathbf{V} \cdot \nabla \end{aligned} \tag{57}$$

These expressions then lead to the demonstration of the invariance of (47). Then in the earth co-moving frame the absolute velocity  $\mathbf{V}$  does not appear in (47). Then another change of variables, as in (37), permits (47) to be written in the form of General Relativity with a Schwarzschild metric.

The consistency between the absolute motion velocity  $\mathbf{V}$  and General Relativity may also be directly checked by showing explicitly, using say *Mathematica*, that the metric

$$d\tau^2 = g_{\mu\nu} dx^\mu dx^\nu = dt^2 - \frac{1}{c^2} (d\mathbf{r}(t) - ((\mathbf{v}(\mathbf{r} - \mathbf{V}t) + \mathbf{V})dt)^2, \tag{58}$$

is a solution to (31) for  $T_{\mu\nu} = 0$ , ie outside matter, where  $\mathbf{v}(\mathbf{r})$  is the in-flow velocity field in (6). This metric is a generalisation of the Panlevé-Gullstrand metric to include the absolute motion effect. This emphasises yet again that for a spherically symmetric matter distribution the Schwarzschild metric, which is equivalent to the Panlevé-Gullstrand metric, is physically identical to Newtonian gravity.

There are nevertheless two differences between the two theories. One is their different treatment of the non-sphericity of the earth via the  $C(\mathbf{v})$  term, and the second difference is the effects of the in-flow turbulence. In the operation of the GPS the density  $\rho(\mathbf{r})$  of the earth is not used. Rather the gravitational potential  $\Phi(\mathbf{r})$  is determined observationally. In the new gravity theory the determination of such a gravitational potential via (47) and  $\Phi(\mathbf{r}) = -\frac{1}{2}\mathbf{v}^2(\mathbf{r})$  would involve the extra  $C(\mathbf{v})$  term. Hence because of this phenomenological treatment the effects of the  $C(\mathbf{v})$  term are not checkable. However the gravitational wave effect is expected to affect the operation of the GPS, and the GPS constellation would

offer a worldwide network which would enable the investigation of the spatial and temporal correlations of these gravitational waves.

There is also a significant interpretational difference between the two theories. For example in General Relativity the relativistic effects involve both the ‘special relativity’ orbital speed effect via time dilations of the satellite clocks together with the General Relativity ‘gravitational potential energy’ effect on the satellite clocks. In the new theory there is only one effect, namely the time dilation effect produced by the motion of the clocks through the quantum foam, and the speeds of these clocks involve the vector sum of the orbital velocity and the velocity caused by the in-flow of the quantum foam into the earth.

The relations in (57) are those of Galilean Relativity. However together with these go the real absolute motion effects of time dilations and length contractions for moving material systems. Then the data from observers in absolute motion may be related by the Lorentz transformation, so long as their data is not corrected for the effects of absolute motion. So the new Process Physics brings together transformations that were, in the past, regarded as mutually exclusive.

## 2.9 Measurements of $G$

As noted in Sect.2.1 Newton’s Inverse Square Law of Gravitation is strictly valid only in cases of spherical symmetry, and then only outside of such a matter distribution. The theory that gravitational effects arise from inhomogeneities in the quantum foam flow implies that there is no ‘universal law of gravitation’ because the inhomogeneities are determined by non-linear ‘fluid equations’ and the solutions have no form which could be described by a ‘universal law’. Fundamentally there is no generic fluid flow behaviour. The Inverse Square Law is then only an approximation, with large deviations expected in the case of spiral galaxies. Nevertheless Newton’s gravitational constant  $G$  will have a definite value as it quantifies the effective rate at which matter dissipates the information content of space.

From these considerations it follows that the measurement of the value of  $G$  will be difficult as the measurement of the forces between two or more objects, which is the usual method of measuring  $G$ , will depend on the geometry of the spatial positioning of these objects in a way not previously accounted for because the Newtonian Inverse Square Law has always been assumed, or in some cases a specified change in the form of the law has been used. But in all cases a ‘law’ has been assumed, and this may have been the flaw in the analysis of data from such experiments. This implies that the value of  $G$  from such experiments will show some variability as a systematic effect has been neglected in analysing the experimental data, for in none of these experiments is spherical symmetry present. So experimental measurements of  $G$  should show an unexpected contextuality. As well the influence of surrounding matter has also not been properly accounted for. Of course any effects of turbulence in the inhomogeneities of the flow has presumably never even been contemplated.

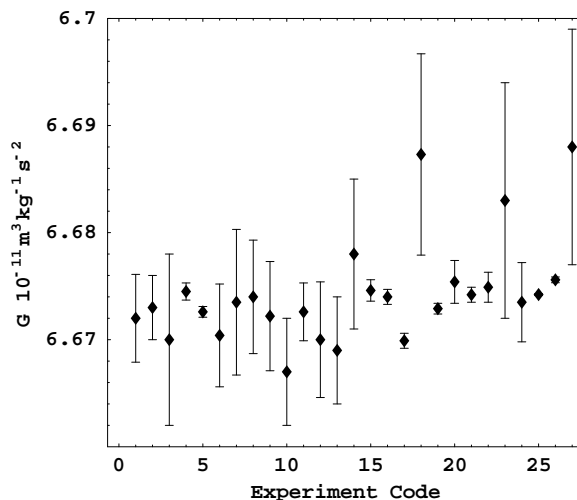


Figure 2: Results of precision measurements of  $G$  published in the last sixty years in which the Newtonian theory was used to analyse the data. These results show the presence of a systematic effect not in the Newtonian theory. **1:** Gaithersburg 1942 [27], **2:** Magny-les-Hameaux 1971 [28], **3:** Budapest 1974 [29], **4:** Moscow 1979 [30], **5:** Gaithersburg 1982 [31], **6-9:** Fribourg Oct 84, Nov 84, Dec 84, Feb 85 [32], **10:** Braunschweig 1987 [33], **11:** Dye 3 Greenland 1995 [34], **12:** Gigerwald Lake 1994 [35], **13-14:** Gigerwald lake 1995 112m, 88m [36], **15:** Lower Hutt 1995 MSL [37], **16:** Los Alamos 1997 [38], **17:** Wuhan 1998 [39], **18:** Boulder JILA 1998 [40], **19:** Moscow 1998 [41], **20:** Zurich 1998 [42], **21:** Lower Hutt MSL 1999 [43], **22:** Zurich 1999 [44], **23:** Sevres 1999 [45], **24:** Wuppertal 1999 [46], **25:** Seattle 2000 [47], **26:** Sevres 2001 [48], **27:** Lake Brasimone 2001 [49]. Data compilation adapted from [50].

The first measurement of  $G$  was in 1798 by Cavendish using a torsional balance. As the precision of experiments increased over the years and a variety of techniques used the disparity between the values of  $G$  has actually increased, as shown in Fig.2, and as reviewed in [51]. In 1998 CODATA increased the uncertainty in  $G$  from 0.013% to 0.15%. One indication of the contextuality is that measurements of  $G$  produce values that differ by nearly 40 times their individual error estimates. It is predicted that these  $G$  anomalies will only be resolved when the new theory of gravity is used in analysing the data from these experiments.

## 2.10 Gravitational Anomalies

In Sect.2.9 anomalies associated with the measurement of  $G$  were briefly discussed and it was pointed out that these were probably explainable within the new in-flow theory of gravity. There are in-fact additional gravitational anomalies that are not well-known in physics, presumably because their existence is incompatible with the Newtonian or the Hilbert-Einstein gravity theories.

The most significant of these anomalies is the Allais effect [53]. In June 1954 Allais<sup>3</sup> reported that a Foucault pendulum exhibited peculiar movements at the time of a solar eclipse. Allais was recording the precession of a Foucault pendulum in Paris. Coincidentally during the 30 day observation period a partial solar eclipse occurred at Paris on June 30. During the eclipse the precession of the pendulum was seen to be disturbed. Similar results were obtained during another solar eclipse on October 29 1959. There have been other repeats of the Allais experiment with varying results.

Another anomaly was reported by Saxl and Allen [54] during the solar eclipse of March 7 1970. Significant variations in the period of a torsional pendulum were observed both during the eclipse and as well in the hours just preceding and just following the eclipse. The effects seem to suggest that an “apparent wavelike structure has been observed over the course of many years at our Harvard laboratory”, where the wavelike structure is present and reproducible even in the absence of an eclipse.

Again Zhou and Huang [55, 56, 57] report various time anomalies occurring during the solar eclipses of September 23 1987, March 18 1988 and July 22 1990 observed using atomic clocks.

Another anomaly is associated with the rotational velocities of objects in spiral galaxies, which are larger than could be maintained by the apparent amount of matter in such galaxies. This anomaly led to the introduction of the ‘dark matter’ concept - but with no such matter ever having been detected, despite extensive searches. This anomaly was compounded when recently observations of the rotational velocities of objects within elliptical galaxies was seen to require very little ‘dark matter’ [58]. Of course this is a simple consequence of the new theory of gravity. The ‘dark matter’ effect is nothing more than an aspect of the self-interaction of space that is absent in both the Newtonian and General Relativity theories. As a system becomes closer to being spherically symmetric, such as in the transition from spiral to elliptical galaxies, the new  $C(\mathbf{v})$  term becomes less effective.

All these anomalies, including the  $g$  anomaly in sect.2.11, and others such as the Pioneer 10/11 de-acceleration anomaly [59] and the solar neutrino flux deficiency problem, not discussed here, would suggest that gravity has aspects to it that are not within the prevailing theories, but that the in-flow theory discussed above might well provide an explanation, and indeed these anomalies may well provide further phenomena that could be used to test the new theory. The effects associated with the solar eclipses could presumably follow from the alignment of the sun, moon and the earth causing enhanced turbulence. The Saxl and Allen experiment of course suggests, like the other experiments, that the turbulence is always present. To explore these anomalies detailed numerical studies of (47) are required with particular emphasis on the effect on the position of the moon.

---

<sup>3</sup>Maurice Allais won the Noble Prize for Economics in 1988.

## 2.11 The Borehole $g$ Anomaly

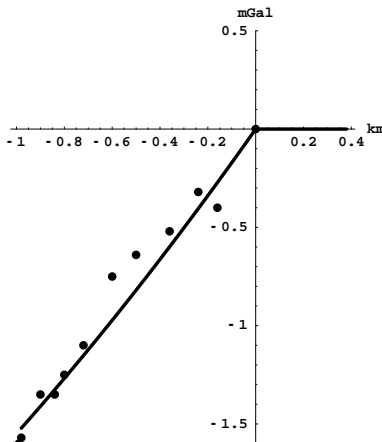


Figure 3: The data shows the gravity residuals for the Hilton mine profile, from Ref.[63], defined as  $\Delta g(r) = g_{Newton} - g_{observed}$ , and measured in mGal ( $1\text{mGal} = 10^{-3} \text{ cm/s}^2$ ) plotted against depth in km. The theory curve shows  $\Delta g(r) = g_{Newton} - g_{InFlow}$  from solving (59) and (60) for a density  $\rho = 2760 \text{ kg/m}^3$  appropriate to the Hilton mine, a coefficient  $\delta = 1$  and  $G = 0.99925G_N$ .

Stacey and others [60, 61, 63] have found evidence for non-Newtonian gravitation from gravimetric measurements (Airy experiments) in mines and boreholes. The discovery was that the measured value of  $g$  down mines and boreholes became greater than that predicted by the Newtonian theory, given the density profile  $\rho(r)$  implied by sampling, and so implying a defect in Newtonian gravity, as shown in Fig.3 for the Hilton mine. The results were interpreted and analysed using either a value of  $G$  different to but larger than that found in laboratory experiments or by assuming a short range Yukawa type force in addition to the Newtonian ‘inverse-square law’. Numerous experiments were carried out in which  $g$  was measured as a function of depth, and also as a function of height above ground level using towers. The tower experiments [64, 65] did not indicate any non-Newtonian effect, and so implied that the extra Yukawa force explanation was not viable. The combined results appeared to have resulted in confusion and eventually the experimental effect was dismissed as being caused by erroneous density sampling [66]. However the new theory of gravity predicts such an effect, and in particular that the effect should manifest within the earth but not above it, as was in fact observed. Essentially this effect is caused by the new  $C(\mathbf{v})$  term in the in-flow theory of gravity which, as we have noted earlier, is active whenever there is a lack of complete spherical symmetry, or even within matter when there is spherical symmetry - this being the case here.

The Newtonian in-flow equation (5) for a time-independent velocity field

becomes for systems with spherical symmetry

$$2\frac{vv'}{r} + (v')^2 + vv'' = -4\pi\rho(r)G_N, \quad (59)$$

where  $v = v(r)$  and  $v' = \frac{dv(r)}{dr}$ . The value of  $v$  at the earth's surface is approximately 11 km/s. This formulation is completely equivalent to the conventional formulation of Newtonian gravity,

In the new gravity theory the in-flow equation (47) has the additional  $C(\mathbf{v})$  term which, in the case of time-independent flows and spherical symmetry, becomes the term in the brackets in (60) with coefficient  $\delta$ ,

$$2\frac{vv'}{r} + (v')^2 + vv'' + \delta\left(\frac{v^2}{2r^2} + \frac{vv'}{r}\right) = -4\pi\rho(r)G. \quad (60)$$

It is important to note that the value of  $G$  is not necessarily the same as the conventional value denoted as  $G_N$ . Both of these equations may be integrated in from the surface, assuming that the in-flow velocity field at or above the surface is given by

$$v(r) = \sqrt{\frac{2G_N M}{r}}, \quad (61)$$

so that it corresponds to the observed surface value of  $g$ . In (59)  $M$  is the total matter content of the earth, but in (60)  $M$  is the sum of the matter content and the effective total 'dark matter' content of the earth. Then above the surface, where  $\rho = 0$ , both flow equations have (61) as identical solutions, since for this velocity field the additional bracketed term in (60) is identically zero. This explains why the tower experiments found no non-Newtonian effects. The in-flow equations may be numerically integrated inward from the surface using as boundary conditions the continuity of  $v(r)$  and  $v'(r)$  at the surface. For each the  $g(r)$  is determined. Fig.3 shows the resulting difference  $\Delta g(r) = g_{Newton} - g_{InFlow}$  compared with the measured anomaly  $\Delta g(r) = g_{Newton} - g_{observed}$ . Assuming  $\delta = 1$  the value of  $G$  was adjusted to agree with the data, giving  $G = 0.99925G_N$ , as shown in Fig.3. However this fit does not uniquely determine the values of  $\delta$  and  $G$ . It should be noted that the data in Fig.3 was adjusted for density irregularities using Newtonian gravity, and this is now seen to be an invalid procedure. Nevertheless the results imply that a repeat of the borehole measurements would be very useful in contributing to the testing of the new theory of gravity, or perhaps even a re-analysis of existing data could be possible. The key signature of the effect, as shown in Fig.3, is the discontinuity in  $d\Delta g(r)/dr$  at the surface, and which is a consequence of having the  $C(\mathbf{v})$  term. Of course using a Yukawa force added to Newtonian gravity cannot produce this key signature, as such a force results in  $d\Delta g(r)/dr$  being continuous at the surface.



## 3 Detection of Absolute Motion and Gravitational Waves

### 3.1 Space and Absolute Motion

Absolute motion is motion relative to space itself. It turns out that Michelson and Morley in their historic experiment of 1887 did detect absolute motion, but rejected their own findings because using their method of analysis of the observed fringe shifts the determined speed of some 8 km/s was less than the 30 km/s orbital speed of the earth. The data was clearly indicating that the theory for the operation of the Michelson interferometer was not adequate. Rather than reaching this conclusion Michelson and Morley came to the incorrect conclusion that their results amounted to the failure to detect absolute motion. This had an enormous impact on the development of physics, for as is well known Einstein adopted the absence of absolute motion effects as one of his fundamental assumptions. By the time Miller had finally figured out how to work around the lack of a viable theory for the operation of the Michelson interferometer, and properly analyse data from his own Michelson interferometer, absolute motion had become a forbidden concept within physics, as it still is at present. The experimental observations by Miller and others of absolute motion has continued to be scorned and rejected by the physics community. Fortunately as well as revealing absolute motion the experimental data also reveals evidence in support of a new theory of gravity.

### 3.2 Theory of the Michelson Interferometer

We now show for the first time in over 100 years how three key effects together permit the Michelson interferometer [17] to reveal the phenomenon of absolute motion when operating in the presence of a gas, with the third effect only discovered in 2002 [8]. The main outcome is the derivation of the origin of the Miller  $k^2$  factor in the expression for the time difference for light travelling via the orthogonal arms,

$$\Delta t = k^2 \frac{L|\mathbf{v}_P|^2}{c^3} \cos(2(\theta - \psi)). \quad (62)$$

Here  $\mathbf{v}_P$  is the projection of the absolute velocity  $\mathbf{v}$  of the interferometer through the quantum-foam onto the plane of the interferometer, where the projected velocity vector  $\mathbf{v}_P$  has azimuth angle  $\psi$  relative to the local meridian, and  $\theta$  is the angle of one arm from that meridian. The  $k^2$  factor is  $k^2 = n(n^2 - 1)$  where  $n$  is the refractive index of the gas through which the light passes,  $L$  is the length of each arm and  $c$  is the speed of light relative to the quantum foam. This expression follows from three key effects: (i) the difference in geometrical length of the two paths when the interferometer is in absolute motion, as first realised

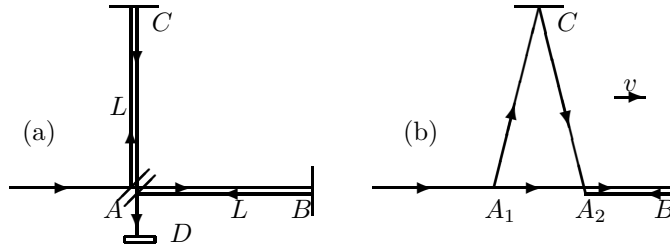


Figure 4: Schematic diagrams of the Michelson Interferometer, with beamsplitter/mirror at  $A$  and mirrors at  $B$  and  $C$ , on equal length arms when parallel, from  $A$ .  $D$  is a quantum detector (not drawn in (b)) that causes localisation of the photon state by a collapse process. In (a) the interferometer is at rest in space. In (b) the interferometer is moving with speed  $v$  relative to space in the direction indicated. Interference fringes are observed at the quantum detector  $D$ . If the interferometer is rotated in the plane through  $90^\circ$ , the roles of arms  $AC$  and  $AB$  are interchanged, and during the rotation shifts of the fringes are seen in the case of absolute motion, but only if the apparatus operates in a gas. By counting fringe changes the speed  $v$  may be determined.

by Michelson, (ii) the Fitzgerald-Lorentz contraction of the arms along the direction of motion, and (iii) that these two effects precisely cancel in vacuum, but leave a residual effect if operated in a gas, because the speed of light through the gas is reduced to  $V = c/n$ , ignoring here for simplicity any Fresnel-drag effects. This is one of the aspects of the quantum foam physics that distinguishes it from the Einstein formalism. The time difference  $\Delta t$  is revealed by the fringe shifts on rotating the interferometer. In Newtonian physics, that is with no Fitzgerald-Lorentz contraction,  $k^2 = n^3$ , while in Einsteinian physics  $k = 0$  reflecting the fundamental assumption that absolute motion is not measurable and indeed has no meaning. So the experimentally determined value of  $k$  is a key test of fundamental physics. For air  $n = 1.00029$ , and so for process physics  $k = 0.0241$  and  $k^2 = 0.00058$ , which is close to the Einsteinian value of  $k = 0$ , particularly in comparison to the Newtonian value of  $k = 1.0$ . This small but non-zero  $k$  value explains why the Michelson interferometer experiments gave such small fringe shifts. Fortunately it is possible to check the  $n$  dependence of  $k$  as two experiments [12, 13] were done in helium gas, and this has an  $n^2 - 1$  value significantly different from that of air.

In deriving (63) in the new physics it is essential to note that space is a quantum-foam system which exhibits various subtle features. In particular it exhibits real dynamical effects on clocks and rods. In this physics the speed of light is only  $c$  relative to the quantum-foam, but to observers moving with respect to this quantum-foam the speed appears to be still  $c$ , but only because their clocks and rods are affected by the quantum-foam. As shown in above such observers will find that records of observations of distant events will be described by the Einstein spacetime formalism, but only if they restrict measurements to

those achieved by using clocks, rods and light pulses, that is using the Einstein measurement protocol. However if they use an absolute motion detector then such observers can correct for these effects.

It is simplest in the new physics to work in the quantum-foam frame of reference. If there is a gas present at rest in this frame, such as air, then the speed of light in this frame is  $V = c/n$ . If the interferometer and gas are moving with respect to the quantum foam, as in the case of an interferometer attached to the earth, then the speed of light relative to the quantum-foam is still  $V = c/n$  up to corrections due to drag effects. Hence this new physics requires a different method of analysis from that of the Einstein physics. With these cautions we now describe the operation of a Michelson interferometer in this new physics, and show that it makes predictions different to that of the Einstein physics. Of course experimental evidence is the final arbiter in this conflict of theories.

As shown in Fig.5 the beamsplitter/mirror when at  $A$  sends a photon  $\psi(t)$  into a superposition  $\psi(t) = \psi_1(t) + \psi_2(t)$ , with each component travelling in different arms of the interferometer, until they are recombined in the quantum detector which results in a localisation process, and one spot in the detector is produced. Repeating with many photons reveals that the interference between  $\psi_1$  and  $\psi_2$  at the detector results in fringes. These fringes actually only appear if the mirrors are not quite orthogonal, otherwise the screen has a uniform intensity and this intensity changes as the interferometer is rotated, as shown in the analysis by Hicks [25]. To simplify the analysis here assume that the two arms are constructed to have the same lengths  $L$  when they are physically parallel to each other and perpendicular to  $v$ , so that the distance  $BB'$  is  $L \sin(\theta)$ . The Fitzgerald-Lorentz effect in the new physics is that the distance  $SB'$  is  $\gamma^{-1}L \cos(\theta)$  where  $\gamma = 1/\sqrt{1 - v^2/c^2}$ . The various other distances are  $AB = Vt_{AB}$ ,  $BC = Vt_{BC}$ ,  $AS = vt_{AB}$  and  $SC = vt_{BC}$ , where  $t_{AB}$  and  $t_{BC}$  are the travel times. Applying the Pythagoras theorem to triangle  $ABB'$  we obtain

$$t_{AB} = \frac{2v\gamma^{-1}L \cos(\theta)}{2(V^2 - v^2)} + \frac{\sqrt{4v^2\gamma^{-2}L^2 \cos^2(\theta) + 4L^2(1 - \frac{v^2}{c^2} \cos^2(\theta))(V^2 - v^2)}}{2(V^2 - v^2)}. \quad (63)$$

The expression for  $t_{BC}$  is the same except for a change of sign of the  $2v\gamma^{-1}L \cos(\theta)$  term, then

$$\begin{aligned} t_{ABC} &= t_{AB} + t_{BC} \\ &= \frac{\sqrt{4v^2\gamma^{-2}L^2 \cos^2(\theta) + 4L^2(1 - \frac{v^2}{c^2} \cos^2(\theta))(V^2 - v^2)}}{(V^2 - v^2)}. \end{aligned} \quad (64)$$

The corresponding travel time  $t'_{ABC}$  for the orthogonal arm is obtained from (64) by the substitution  $\cos(\theta) \rightarrow \cos(\theta + 90^\circ) = -\sin(\theta)$ . The difference in travel

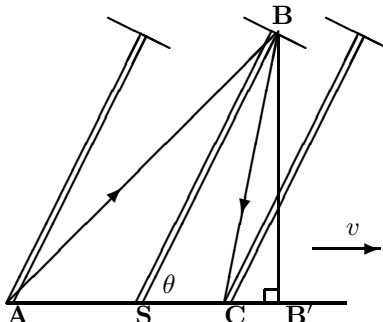


Figure 5: One arm of a Michelson Interferometer travelling at angle  $\theta$  and velocity  $\mathbf{v}$ , and shown at three successive times: (i) when photon leaves beamsplitter at A, (ii) when photon is reflected at mirror B, and (iii) when photon returns to beamsplitter at C. The line  $BB'$  defines right angle triangles  $ABB'$  and  $SBB'$ . The second arm is not shown but has angle  $\theta + 90^\circ$  to  $\mathbf{v}$ . Here  $\mathbf{v}$  is in the plane of the interferometer for simplicity, and the azimuth angle  $\psi = 0$ .

times between the two arms is then  $\Delta t = t_{ABC} - t'_{ABC}$ . Now trivially  $\Delta t = 0$  if  $v = 0$ , but also  $\Delta t = 0$  when  $v \neq 0$  but only if  $V = c$ . This then would result in a null result on rotating the apparatus. Hence the null result of Michelson interferometer experiments in the new physics is only for the special case of photons travelling in vacuum for which  $V = c$ . However if the interferometer is immersed in a gas then  $V < c$  and a non-null effect is expected on rotating the apparatus, since now  $\Delta t \neq 0$ . It is essential then in analysing data to correct for this refractive index effect. The above  $\Delta t$  is the change in travel time when one arm is moved through angle  $\theta$ . The interferometer operates by comparing the change in the difference of the travel times between the arms. Then for  $V = c/n$  we find for  $v \ll V$  that

$$\Delta t = Ln(n^2 - 1) \frac{v^2}{c^3} \cos(2\theta) + O(v^4), \quad (65)$$

that is  $k^2 = n(n^2 - 1)$ , which gives  $k = 0$  for vacuum experiments ( $n = 1$ ). So the Miller phenomenological parameter  $k$  is seen to accommodate both the Fitzgerald-Lorentz contraction effect and the dielectric effect, at least for gases. This is very fortunate since being a multiplicative parameter a re-scaling of old analyses is all that is required.  $\Delta t$  is non-zero when  $n \neq 1$  because the refractive index effect results in incomplete cancellation of the geometrical effect and the Fitzgerald-Lorentz contraction effect. Of course it was this cancellation effect that Fitzgerald and Lorentz actually used to arrive at the length contraction hypothesis, but they failed to take the next step and note that the cancellation would be incomplete in the air operated Michelson-Morley experiment. In a bizarre development modern Michelson interferometer experiments, which use resonant cavities rather than interference effects, but for which the analysis here is easily adapted, and with the same consequences, are operated in vacuum

mode. That denies these experiments the opportunity to see absolute motion effects. Nevertheless the experimentalists continue to misinterpret their null results as evidence against absolute motion. Of course these experiments are therefore restricted to merely checking the Fitzgerald-Lorentz contraction effect, and this is itself of some interest.

All data from gas-mode interferometer experiments, except for that of Miller, has been incorrectly analysed using only the first effect as in Michelson's initial theoretical treatment, and so the consequences of the other two effects have been absent. Repeating the above analysis without these two effects we arrive at the Newtonian-physics time difference which, for  $v \ll V$ , is

$$\Delta t = Ln^3 \frac{v^2}{c^3} \cos(2\theta) + O(v^4), \quad (66)$$

that is  $k^2 = n^3$ . The value of  $\Delta t$ , which is typically of order  $10^{-17}s$  in gas-mode interferometers corresponding to a fractional fringe shift, is deduced from analysing the fringe shifts, and then the speed  $v_M$  has been extracted using (66), instead of the correct form (65) or more generally (63). However it is very easy to correct for this oversight. From (65) and (66) we obtain for the corrected absolute (projected) speed  $v_P$  through space, and for  $n \approx 1^+$ ,

$$v_P = \frac{v_M}{\sqrt{n^2 - 1}}. \quad (67)$$

For air the correction factor in (67) is significant, and even more so for helium.

### 3.3 The Michelson-Morley Experiment: 1887

Michelson and Morley reported that their interferometer experiment in 1887 gave a 'null-result' which since then, with rare exceptions, has been claimed to support the Einstein assumption that absolute motion has no meaning. However to the contrary the Michelson-Morley published data [10] shows non-null effects, but much smaller than they expected. They made observations of thirty-six  $360^0$  turns using an  $L = 11$  meter length interferometer, achieved using multiple reflections, operating in air in Cleveland (Latitude  $41^030'N$ ) with six turns near 12:00 hrs (7:00 hrs ST) on each day of July 8, 9 and 11, 1887 and similarly near 18:00 hrs (13:00 hrs ST) on July 8, 9 and 12, 1887. Each turn took approximately 6 minutes as the interferometer slowly rotated floating on a tank of mercury. They published and analysed the average of each of the 6 data sets. The fringe shifts were extremely small but within their observational capabilities.

Table 2 shows examples of the averaged fringe shift micrometer readings every  $22.5^0$  of rotation of the Michelson-Morley interferometer [10] for July 11 12:00 hr local time and also for July 9 18:00 hr local time. The orientation of the stone slab base is indicated by the marks 16, 1, 2, ... North is mark 16. The dominant effect was a uniform fringe drift caused by temporal temperature effects on the length of the arms, and imposed upon that are the fringe shifts corresponding to the effects of absolute motion, as shown in Fig.6.

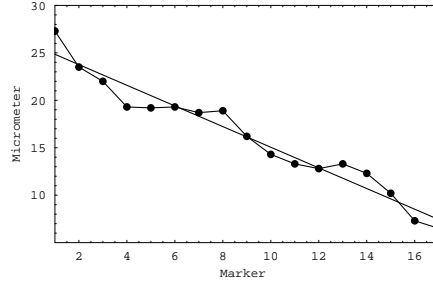


Figure 6: Plot of micrometer readings for July 11 12:00 hr (7:00 ST) showing the absolute motion induced fringe shifts superimposed on the uniform temperature induced fringe drift. Most physics books deny that these fringe shifts were seen, despite being available in [10].

local time	16 8	1 9	2 10	3 11	4 12	5 13	6 14	7 15	16
12:00hr	27.3	23.5	22.0	19.3	19.2	19.3	18.7	18.9	
July 11	16.2	14.3	13.3	12.8	13.3	12.3	10.2	7.3	6.5
18:00hr	26.0	26.0	28.2	29.2	31.5	32.0	31.3	31.7	
July 9	33.0	35.8	36.5	37.3	38.8	41.0	42.7	43.7	44.0

Table 2. Examples of Michelson-Morley fringe-shift micrometer readings, from [10]. The readings for July 11 12:00 hr are plotted in Fig.6.

This temperature effect can be removed by subtracting from the data in each case a best fit to the data of  $a + bk$ ,  $\{k = 0, 1, 2, \dots, 8\}$  for the first  $0^\circ$  to  $180^\circ$  part of each rotation data set. Then multiplying by 0.02 for the micrometer thread calibration gives the fringe-shift data points in Fig.8. This factor of 0.02 converts the micrometer readings to fringe shifts expressed as fractions of a wavelength. Similarly a linear fit has been made to the data from the  $180^\circ$  to  $360^\circ$  part of each rotation data set. Separating the full  $360^\circ$  rotation into two  $180^\circ$  parts reduces the effect of the temperature drift not being perfectly linear in time.

In the new physics there are four main velocities that contribute to the total velocity:

$$\mathbf{v} = \mathbf{v}_{cosmic} + \mathbf{v}_{tangent} - \mathbf{v}_{in} - \mathbf{v}_E. \quad (68)$$

Here  $\mathbf{v}_{cosmic}$  is the velocity of the solar system relative to some cosmologically defined galactic quantum-foam system (discussed later) while the other three are local effects: (i)  $\mathbf{v}_{tangent}$  is the tangential orbital velocity of the earth about the sun, (ii)  $\mathbf{v}_{in}$  is a quantum-gravity radial in-flow of the quantum foam past the earth towards the sun, and (iii) the corresponding quantum-foam in-flow into the earth is  $\mathbf{v}_E$  and makes no contribution to a horizontally operated interferometer, assuming the velocity superposition approximation, and also that the turbulence associated with that flow is not significant. The minus signs in

(68) arise because, for example, the in-flow towards the sun requires the earth to have an outward directed velocity against that in-flow in order to maintain a fixed distance from the sun, as shown in Fig.7. For circular orbits and using in-flow form of Newtonian gravity the speeds  $v_{tangent}$  and  $v_{in}$  are given by

$$v_{tangent} = \sqrt{\frac{GM}{R}}, \quad (69)$$

$$v_{in} = \sqrt{\frac{2GM}{R}}, \quad (70)$$

while the net speed  $v_R$  of the earth from the vector sum  $\mathbf{v}_R = \mathbf{v}_{tangent} - \mathbf{v}_{in}$  is

$$v_R = \sqrt{\frac{3GM}{R}}, \quad (71)$$

where  $M$  is the mass of the sun,  $R$  is the distance of the earth from the sun, and  $G$  is Newton's gravitational constant.  $G$  is essentially a measure of the rate at which matter effectively 'dissipates' the quantum-foam. The gravitational acceleration arises from inhomogeneities in the flow. These expressions give  $v_{tangent} = 30\text{km/s}$ ,  $v_{in} = 42.4\text{km/s}$  and  $v_R = 52\text{km/s}$ .

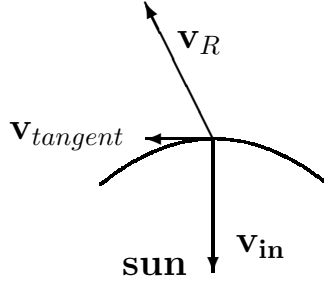


Figure 7: Orbit of earth about the sun defining the plane of the ecliptic with tangential orbital velocity  $\mathbf{v}_{tangent}$  and quantum-foam in-flow velocity  $\mathbf{v}_{in}$ . Then  $\mathbf{v}_R = \mathbf{v}_{tangent} - \mathbf{v}_{in}$  is the velocity of the earth relative to the quantum foam, after subtracting  $\mathbf{v}_{cosmic}$ .

Fig.8 shows all the data for the 1887 Michelson-Morley experiment for the fringe shifts after removal of the temperature drift effect for each averaged 180 degree rotation. The dotted curves come from the best fit of  $\frac{0.4}{30^2} k_{air}^2 v_P^2 \cos(2(\theta - \psi))$  to the data. The coefficient  $0.4/30^2$  arises as the apparatus would give a 0.4 fringe shift, as a fraction of a wavelength, with  $k = 1$  if  $v_P = 30$  km/s [10]. Shown in each figure is the resulting value of  $v_P$ . In some cases the data does not have the expected  $\cos(2(\theta - \psi))$  form, and so the corresponding values for  $v_P$  are not meaningful. The remaining fits give  $v_P = 331 \pm 30$  km/s for the 7:00 hr (ST) data, and  $v_P = 328 \pm 50$  km/s for the 13:00 hr (ST) data. For comparison the full curves show the predicted form for the Michelson-Morley data, computed for the latitude of Cleveland, using the Miller direction

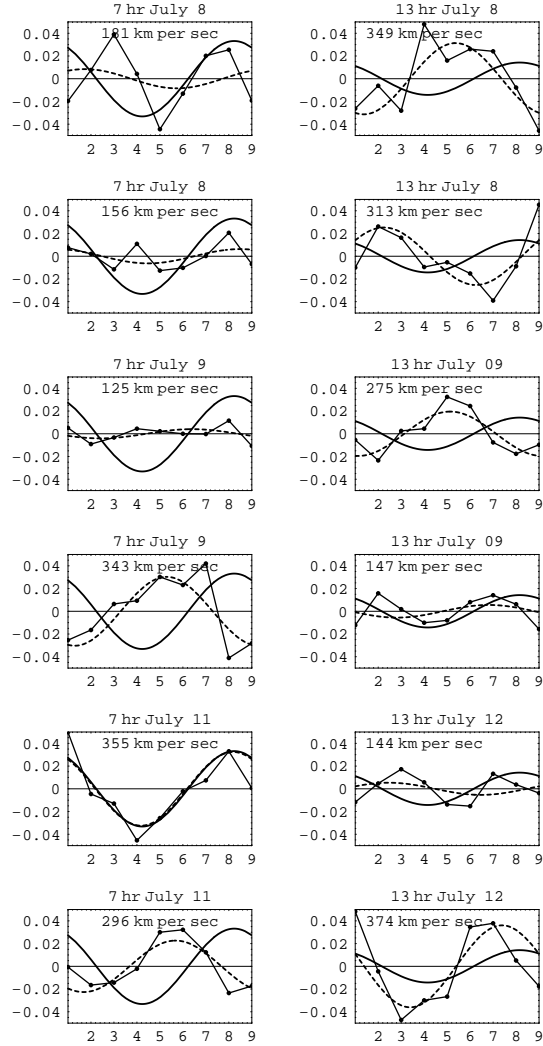


Figure 8: Shows all the Michelson-Morley 1887 data after removal of the temperature induced fringe drifts. The data for each  $360^\circ$  full turn (the average of 6 individual turns) is divided into the 1st and 2nd  $180^\circ$  parts and plotted one above the other. The dotted curve shows a best fit to the data, while the full curves show the expected forms using the Miller direction for  $\mathbf{v}_{cosmic}$ .



(see later) for  $\mathbf{v}_{cosmic}$  of Right Ascension and Declination ( $\alpha = 4^{hr}54', \delta = -70^{\circ}30'$ ) and incorporating the tangential and in-flow velocity effects for July. The magnitude of the theoretical curves are in general in good agreement with the magnitudes of the experimental data, excluding those cases where the data does not have the sinusoidal form. However there are significant fluctuations in the azimuth angle. These fluctuations are also present in the Miller data, and together suggest that this is a real physical phenomenon, and not solely due to difficulties with the operation of the interferometer.

The Michelson-Morley interferometer data clearly shows the characteristic sinusoidal form with period  $180^{\circ}$  together with a large speed. Ignoring the effect of the refractive index, namely using the Newtonian value of  $k = 1$ , gives speeds reduced by the factor  $k_{air}$ , namely  $k_{air}v_P = 0.0241 \times 330\text{km/s} = 7.9 \text{ km/s}$ . Michelson and Morley reported speeds in the range  $5\text{km/s} - 7.5\text{km/s}$ . These slightly smaller speeds arise because they averaged all the 7:00 hr (ST) data, and separately all the 13:00 hr (ST) data, whereas here some of the lower quality data have not been used. Michelson was led to the false conclusion that because this speed of some  $8 \text{ km/s}$  was considerably less than the orbital speed of  $30 \text{ km/s}$  the interferometer must have failed to have detected absolute motion, and that the data was merely caused by experimental imperfections. This was the flawed analysis that led to the incorrect conclusion by Michelson and Morley that the experiment had failed to detect absolute motion. The consequences for physics were extremely damaging, and are only now being rectified after some 115 years.

### 3.4 The Miller Interferometer Experiment: 1925-1926

Dayton Miller developed and operated a Michelson interferometer for over twenty years, with the main sequence of observations being on Mt. Wilson in the years 1925-1926, with the results reported in 1933 by Miller [11]. Accounts of the Miller experiments are available in Swenson [52]. Miller developed his huge interferometer over the years, from 1902 to 1906, in collaboration with Morley, and later at Mt. Wilson where the most extensive interferometer observations were carried out. Miller was meticulous in perfecting the operation of the interferometer and performed many control experiments. The biggest problem to be controlled was the effect of temperature changes on the lengths of the arms. It was essential that the temperature effects were kept as small as possible, but so long as each turn was performed sufficiently quickly, any temperature effect could be assumed to have been linear with respect to the angle of rotation. Then a uniform background fringe drift could be removed, as in the Michelson-Morley data analysis (see Fig.6).

In all some 200,000 readings were taken during some 12,000 turns of the interferometer<sup>4</sup>. Analysis of the data requires the extraction of the speed  $v_M$

<sup>4</sup>In a remarkable development in 2002 as a result of a visit by James DeMeo to Case Western Reserve University the original Miller data was located, some 61 years after Miller's death in 1941. Until then it was thought that the data had been destroyed. Analysis of that

and the azimuth angle  $\psi$  by effectively fitting the observed time differences, obtained from the observed fringe shifts, using (63), but with  $k = 1$ . Miller was of course unaware of the full theory of the interferometer and so he assumed the Newtonian theory, which neglected both the Fitzgerald-Lorentz contraction and air effects.

Miller performed his observations in April, August and September 1925 and February 1926 and the data is shown in Figs.9 and 11. The speeds shown are the Michelson speeds  $v_M$ , and these are easily corrected for the two neglected effects by dividing these  $v_M$  by  $k_{air} = \sqrt{(n^2 - 1)} = 0.0241$ , as in (67). Then for example a speed of  $v_M = 10\text{km/s}$  gives  $v_P = v_M/k_{air} = 415\text{km/s}$ . However this correction procedure was not available to Miller. He understood that the theory of the Michelson interferometer was not complete, and so he introduced the phenomenological parameter  $k$  in (63). We shall denote his values by  $\bar{k}$ . Miller noted, in fact, that  $\bar{k}^2 \ll 1$ , as we would now expect. Miller then proceeded on the assumption that  $\mathbf{v}$  should have only two components: (i) a cosmic velocity of the solar system through space, and (ii) the orbital velocity of the earth about the sun. Over a year this vector sum would result in a changing  $\mathbf{v}$ , as was in fact observed. Further, since the orbital speed was known, Miller was able to extract from the data the magnitude and direction of  $\mathbf{v}$  as the orbital speed offered an absolute scale. For example the dip in the  $v_M$  plots for sidereal times  $\tau \approx 16^{hr}$  is a clear indication of the direction of  $\mathbf{v}$ , as the dip arises at those sidereal times when the projection  $v_P$  of  $\mathbf{v}$  onto the plane of the interferometer is at a minimum. During a 24hr period the value of  $v_P$  varies due to the earth's rotation. As well the  $v_M$  plots vary throughout the year because the vectorial sum of the earth's orbital velocity  $\mathbf{v}_{tangent}$  and the cosmic velocity  $\mathbf{v}_{cosmic}$  changes. There are two effects here as the direction of  $\mathbf{v}_{tangent}$  is determined by both the yearly progression of the earth in its orbit about the sun, and also because the plane of the ecliptic is inclined at  $23.5^\circ$  to the celestial plane. Figs.9 and 11 show the expected theoretical variation of both  $v_P$  and the azimuth  $\psi$  during one sidereal day in the months of April, August, September and February. These plots show the clear signature of absolute motion effects as seen in the actual interferometer data.

Note that the above corrected Miller projected absolute speed of approximately  $v_P = 415\text{km/s}$  is completely consistent with the corrected projected absolute speed of some  $330\text{km/s}$  from the Michelson-Morley experiment, though neither Michelson nor Miller were able to apply this correction. The difference in magnitude is completely explained by Cleveland having a higher latitude than Mt. Wilson, and also by the only two sidereal times of the Michelson-Morley observations. So from his 1925-1926 observations Miller had completely confirmed the true validity of the Michelson-Morley observations and was able to conclude, contrary to their published conclusions, that the 1887 experiment had in fact detected absolute motion. But it was too late. By then the physicists had incorrectly come to believe that absolute motion was inconsistent with

---

data by the author of this article has confirmed the accuracy of Miller's analysis. Using more thorough computer based techniques the data is now being re-analysed.

various ‘relativistic effects’ that had by then been observed. This was because the Einstein formalism had been ‘derived’ from the assumption that absolute motion was without meaning and so unobservable in principle. Of course the earlier interpretation of relativistic effects by Lorentz had by then lost out to the Einstein interpretation.

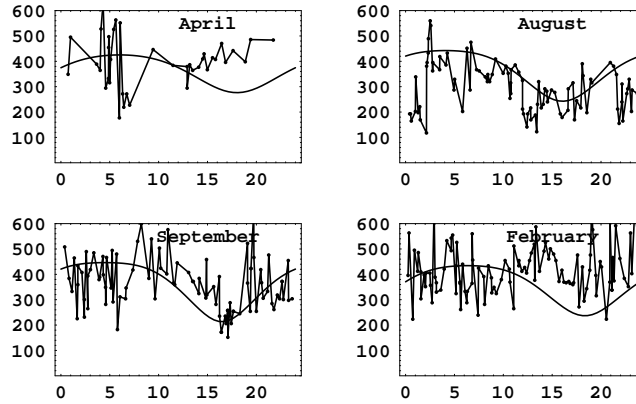


Figure 9: Miller interferometer projected speeds  $v_P$  in km/s showing both data and best fit of theory giving  $v_{cosmic} = 433$  km/s in the direction ( $\alpha = 5.2^{hr}$ ,  $\delta = -67^0$ ), and using  $n = 1.000226$  appropriate for the altitude of Mt. Wilson

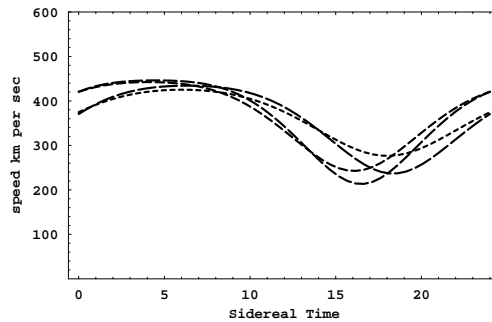


Figure 10: Expected theoretical variation of the projected velocity  $v_P$  during one sidereal day in the months of April, August, September and February, labelled by increasing dash length for cosmic speed of 433km/s in the direction ( $\alpha = 5.2^{hr}$ ,  $\delta = -67^0$ ). This shows the signature of the earth’s orbital rotation.

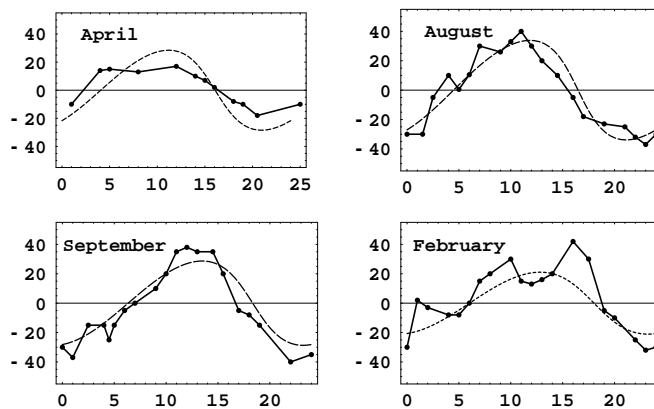


Figure 11: Running time-averaged Miller azimuths  $\psi$ , in degrees, measured from south, showing both data and best fit of theory giving  $v_{cosmic} = 433$  km/s in the direction ( $\alpha = 5.2^{hr}$ ,  $\delta = -67^0$ ), and using  $n = 1.000226$ .

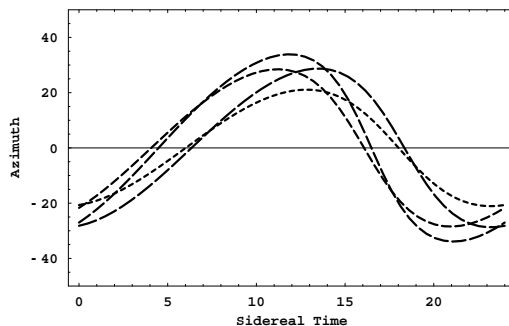


Figure 12: Expected theoretical variation of the azimuths  $\psi$ , measured from south, during one sidereal day in the months of April, August, September and February, labelled by increasing dash length, for a cosmic speed of 433km/s in the direction ( $\alpha = 5.2^{hr}$ ,  $\delta = -67^0$ ). This shows the signature of the earth's orbital rotation.

### 3.5 Gravitational In-flow from the Miller Data

As already noted Miller was led to the conclusion that for reasons unknown the existing theory of the Michelson interferometer did not reveal true values of  $v_P$ , and for this reason he introduced the parameter  $k$ , with  $\bar{k}$  indicating his numerical values. Miller had reasoned that he could determine both  $\mathbf{v}_{cosmic}$  and  $\bar{k}$  by observing the interferometer determined  $v_P$  and  $\psi$  over a year because the known orbital velocity of the earth about the sun would modulate both of these

observables, and by a scaling argument he could determine the absolute velocity of the solar system. In this manner he finally determined that  $|\mathbf{v}_{cosmic}| = 208$  km/s in the direction ( $\alpha = 4^{hr}54^m, \delta = -70^033'$ ). However now that the theory of the Michelson interferometer has been revealed an anomaly becomes apparent. Table 3 shows  $v = v_M/k_{air}$  for each of the four epochs, giving speeds consistent with the revised Michelson-Morley data. However Table 3 also shows that  $\bar{k}$  and the speeds  $\bar{v} = v_M/\bar{k}$  determined by the scaling argument are considerably different. Here the  $v_M$  values arise after taking account of the projection effect. That  $\bar{k}$  is considerably larger than the value of  $k_{air}$  indicates that another velocity component has been overlooked. Miller of course only knew of the tangential orbital speed of the earth, whereas the new physics predicts that as-well there is a quantum-gravity radial in-flow  $\mathbf{v}_{in}$  of the quantum foam. We can re-analyse Miller's data to extract a first approximation to the speed of this in-flow component. Clearly it is  $v_R = \sqrt{v_{in}^2 + v_{tangent}^2}$  that sets the scale and not  $v_{tangent}$ , and because  $\bar{k} = v_M/v_{tangent}$  and  $k_{air} = v_M/v_R$  are the scaling relations, then

$$\begin{aligned} v_{in} &= v_{tangent} \sqrt{\frac{v_R^2}{v_{tangent}^2} - 1}, \\ &= v_{tangent} \sqrt{\frac{\bar{k}^2}{k_{air}^2} - 1}. \end{aligned} \tag{72}$$

Using the  $\bar{k}$  values in Table 3 and the value<sup>5</sup> of  $k_{air}$  we obtain the  $v_{in}$  speeds shown in Table 3, which give an average speed of 54 km/s, compared to the 'Newtonian' in-flow speed of 42 km/s. Note that the in-flow interpretation of the anomaly predicts that  $\bar{k} = (v_R/v_{tangent}) k_{air} = \sqrt{3} k_{air} = 0.042$ . Of course this simple re-scaling of the Miller results is not completely valid because (i) the direction of  $\mathbf{v}_R$  is of course different to that of  $\mathbf{v}_{tangent}$ , and also not necessarily orthogonal to  $\mathbf{v}_{tangent}$  because of turbulence, and (ii) also because of turbulence we would expect some contribution from the in-flow effect of the earth itself, namely that it is not always perpendicular to the earth's surface, and so would give a contribution to a horizontally operated interferometer.

An analysis that properly searches for the in-flow velocity effect clearly requires a complete re-analysis of the Miller data, and this is now possible and underway at Flinders University as the original data sheets have been found. It should be noted that the direction approximately diametrically opposite ( $\alpha = 4^{hr}54^m, \delta = -70^033'$ ), namely ( $\alpha = 17^{hr}, \delta = +68'$ ) was at one stage considered by Miller as being possible. This is because the Michelson interferometer, being a 2nd-order device, has a directional ambiguity which can only be resolved by using the seasonal motion of the earth. However as Miller did not

<sup>5</sup>In this section we have not modified this value to take account of the altitude effect or temperatures atop Mt.Wilson. This weather information was not recorded by Miller. The temperature and pressure effect is that  $n = 1.0 + 0.00029 \frac{P}{P_0} \frac{T_0}{T}$ , where  $T$  is the temperature in  $^0K$  and  $P$  is the pressure in atmospheres.  $T_0 = 273K$  and  $P_0 = 1atm$ .

Epoch	$v_M$	$\bar{k}$	$v = v_M/k_{air}$	$\bar{v} = v_M/\bar{k}$	$v = \sqrt{3}\bar{v}$	$v_{in}$
February	9.3	0.048	385.9	193.8	335.7	51.7
April	10.1	0.051	419.1	198.0	342.9	56.0
August	11.2	0.053	464.7	211.3	366.0	58.8
September	9.6	0.046	398.3	208.7	361.5	48.8

Table 3. The  $\bar{k}$  anomaly,  $\bar{k} \gg k_{air} = 0.0241$ , as the gravitational in-flow effect. Here  $v_M$  and  $\bar{k}$  come from fitting the interferometer data, while  $v$  and  $\bar{v}$  are computed speeds using the indicated scaling. The average of the in-flow speeds is  $v_{in} = 54 \pm 5$  km/s, compared to the ‘Newtonian’ in-flow speed of 42 km/s. From column 4 we obtain the average  $v = 417 \pm 40$ km/s. All speeds in table in km/s.

include the in-flow velocity effect in his analysis it is possible that a re-analysis might give this northerly direction as the direction of absolute motion of the solar system.

Hence not only did Miller observe absolute motion, as he claimed, but the quality and quantity of his data has also enabled the confirmation of the existence of the gravitational in-flow effect. This is a manifestation of a new theory of gravity and one which relates to quantum gravitational effects via the unification of matter and space. As well the persistent evidence that this in-flow is turbulent indicates that this theory of gravity involves self-interaction of space itself.

### 3.6 The Illingworth Experiment: 1927

In 1927 Illingworth [12] performed a Michelson interferometer experiment in which the light beams passed through the gas helium,

*...as it has such a low index of refraction that variations due to temperature changes are reduced to a negligible quantity.*

For helium at STP  $n = 1.000036$  and so  $k_{He}^2 = 0.00007$ , which results in an enormous reduction in sensitivity of the interferometer. Nevertheless this experiment gives an excellent opportunity to check the  $n$  dependence in (67). Illingworth, not surprisingly, reported no “ether drift to an accuracy of about one kilometer per second”. Múnera [?] re-analysed the Illingworth data to obtain a speed  $v_M = 3.13 \pm 1.04$ km/s. The correction factor in (67),  $1/\sqrt{n_{He}^2 - 1} = 118$ , is large for helium and gives  $v = 368 \pm 123$ km/s. As shown in Fig.13 the Illingworth observations now agree with those of Michelson-Morley and Miller, though they would certainly be inconsistent without the  $n$ -dependent correction, as shown in the lower data points (shown at  $5 \times$  scale).

So the use by Illingworth of helium gas, and also by Joos, has turned out have offered a fortuitous opportunity to confirm the validity of the refractive index effect, though because of the insensitivity of this experiment the resulting error range is significantly larger than those of the other interferometer observations. So finally it is seen that the Illingworth experiment detected absolute motion with a speed consistent with all other observations.

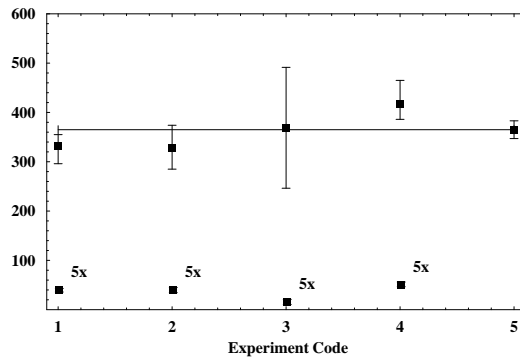


Figure 13: Speeds  $v$  in km/s determined from various Michelson interferometer experiments (1)-(4) and CMB (5): (1) Michelson-Morley (noon observations) and (2) (18<sup>h</sup> observations) see Sect.3.3, (3) Illingworth [12], (4) Miller, Mt.Wilson [11], and finally in (5) the speed from observations of the CMB spectrum dipole term [22]. The results (1)-(3) are not corrected for the  $\pm 30$ km/s of the orbital motion of the earth about the sun for the gravitational in-flow speed, though these corrections were made for (4) with the speeds from Table 3. The horizontal line at  $v = 369$ km/s is to aid comparisons with the CMB frame speed data. The Miller direction is different to the CMB direction. Due to the angle between the velocity vector and the plane of interferometer the results (1)-(3) are less than or equal to the true speed, while the result for (4) is the true speed as this projection effect was included in the analysis. These results demonstrate the remarkable consistency between the three interferometer experiments. The Miller speed agrees with the speed from the DeWitte non-interferometer experiment, in Sect.3.9. The lower data, magnified by a factor of 5, are the original speeds  $v_M$  determined from fringe shifts using (62) with  $k = 1$ . This figure updates the corresponding figure in Ref.[8].

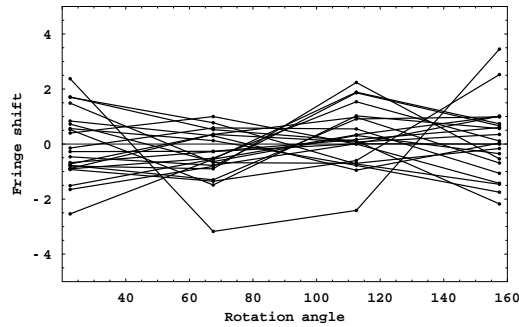


Figure 14: The Joos fringes shifts in  $\lambda/1000$  recorded on May 30, 1930 from a Michelson interferometer using helium. Only one of the rotations produced a clean signal of the form expected.

### 3.7 The Joos Experiment: 1930

Joos set out to construct and operate a large vacuum Michelson interferometer at the Zeiss Works in Jena, Germany 1930 [13]. This interferometer had an effective arm length of 10.5m achieved using multiple reflections in each arm. The vacuum sealing was ineffective and the penetration of air into the vacuum vessel caused problematic vibrations. Subsequently Joos used helium, assuming apparently that helium could be considered as a substitute for a true vacuum<sup>6</sup>. The use of helium is not mentioned in the Joos paper [13], but is mentioned by Swenson [52]. Joos recorded the fringe shifts photographically, and subsequently analysed the images using a photometer. The data for 22 rotations throughout the day of May 30, 1930 are shown in Fig.14, and are reproduced from Fig.11 of [13]. From that data Joos concluded, using an analysis that did not take account of the special relativistic length contraction effect, that the fringe shifts corresponded to a speed of only 1.5 km/s. However as previously noted such an analysis is completely flawed. As well the data in Fig.14 shows that for all but one of the rotations the fringe shifts were poorly recorded. Only in the one rotation, at 11 23<sup>58</sup>, does the data actually look like the form expected. This is probably not accidental as the maximum fringe shift was expected at that time, based on the Miller direction of absolute motion, and the sensitivity of the device was  $\pm 1$  thousandth of a fringe shift. In Fig.15 that one rotation data is compared with the form expected for Jena on May 30 using the Miller speed and direction together with the new refractive index effect, and using the refractive index of helium. The agreement is quite remarkable. So again contrary the Joos paper and to subsequent commentators Joos did in fact detect a very large velocity of absolute motion.

<sup>6</sup>Thanks to Dr Lance McCarthy for pointing out the use of helium in this experiment and in extracting the data from the Joos paper.



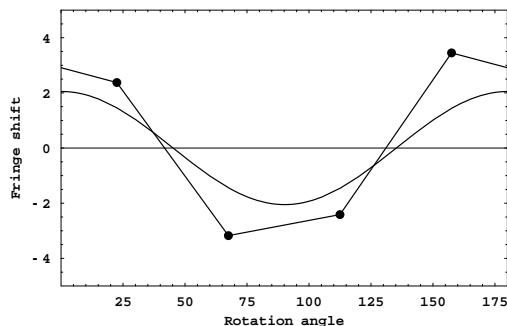


Figure 15: Comparison of the Joos data for the one good rotation at 11 23<sup>58</sup> with the theoretical prediction using the speed and direction from the Miller experiment, together with the length contraction and refractive index effects. The device sensitivity was  $\pm 1$ .

### 3.8 The New Bedford Experiment: 1963

In 1964 from an absolute motion detector experiment at New Bedford, latitude  $42^{\circ}\text{N}$ , Jaseja *et al* [14] reported yet another ‘null result’. In this experiment two He-Ne masers were mounted with axes perpendicular on a rotating table, see Fig.16. Rotation of the table through  $90^{\circ}$  produced repeatable variations in the frequency difference of about 275kHz, an effect attributed to magnetorestriction in the Invar spacers due to the earth’s magnetic field. Observations over some six consecutive hours on January 20, 1963 from 6:00 am to 12:00 noon local time did produce a ‘dip’ in the frequency difference of some 3kHz superimposed on the 275kHz effect, as shown in Fig.17 in which the local times have been converted to sidereal times. The most noticeable feature is that the dip occurs at approximately 17 – 18:00<sup>hr</sup> sidereal time (or 9 – 10:00 hrs local time), which agrees with the direction of absolute motion observed by Miller and also by DeWitte (see Sect.3.9). It was most fortunate that this particular time period was chosen as at other times the effect is much smaller, as shown for example for the February data in Fig.9 which shows the minimum at 18:00<sup>hr</sup> sidereal time. The local times were chosen by Jaseja *et al* such that if the only motion was due to the earth’s orbital speed the maximum frequency difference, on rotation, should have occurred at 12:00hr local time, and the minimum frequency difference at 6:00 hr local time, whereas in fact the minimum frequency difference occurred at 9:00 hr local time.

As for the Michelson-Morley experiment the analysis of the New Bedford experiment was also bungled. Again this apparatus can only detect the effects of absolute motion if the cancellation between the geometrical effects and Fitzgerald-Lorentz length contraction effects is incomplete as occurs only when the radiation travels in a gas, here the He-Ne gas present in the maser.

This double maser apparatus is essentially equivalent to a Michelson interferometer. Then the resonant frequency  $\nu$  of each maser is proportional to the

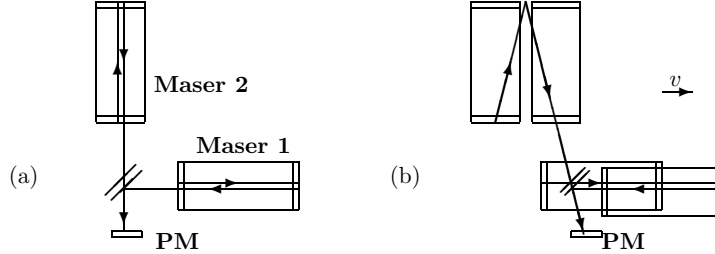


Figure 16: Schematic diagram for recording the variations in beat frequency between two optical masers: (a) when at absolute rest, (b) when in absolute motion at velocity  $\mathbf{v}$ . PM is the photomultiplier detector. The apparatus was rotated back and forth through  $90^\circ$ .

reciprocal of the out-and-back travel time. For maser 1

$$\nu_1 = m \frac{V^2 - v^2}{2LV \sqrt{1 - \frac{v^2}{c^2}}}, \quad (73)$$

for which a Fitzgerald-Lorentz contraction occurs, while for maser 2

$$\nu_2 = m \frac{\sqrt{V^2 - v^2}}{2L}. \quad (74)$$

Here  $m$  refers to the mode number of the masers. When the apparatus is rotated the net observed frequency difference is  $\delta\nu = 2(\nu_2 - \nu_1)$ , where the factor of ‘2’ arises as the roles of the two masers are reversed after a  $90^\circ$  rotation. Putting  $V = c/n$  we find for  $v \ll V$  and with  $\nu_0$  the at-rest resonant frequency, that

$$\delta\nu = (n^2 - 1)\nu_0 \frac{v^2}{c^2} + O\left(\frac{v^4}{c^4}\right). \quad (75)$$

If we use the Newtonian physics analysis, as in Jaseja *et al* [14], which neglects both the Fitzgerald-Lorentz contraction and the refractive index effect, then we obtain  $\delta\nu = \nu_0 v^2/c^2$ , that is without the  $n^2 - 1$  term, just as for the Newtonian analysis of the Michelson interferometer itself. Of course the very small magnitude of the absolute motion effect, which was approximately 1/1000 that expected assuming only an orbital speed of  $v = 30$  km/s in the Newtonian analysis, occurs simply because the refractive index of the He-Ne gas is very close to one<sup>7</sup>. Nevertheless given that it is small the sidereal time of the obvious ‘dip’ coincides almost exactly with that of the other observations of absolute motion.

The New Bedford experiment was yet another missed opportunity to have revealed the existence of absolute motion. Again the spurious argument was that

<sup>7</sup>It is possible to compare the refractive index of the He-Ne gas mixture in the maser with the value extractable from this data:  $n^2 = 1 + 30^2/(1000 \times 400^2)$ , or  $n = 1.0000028$ .

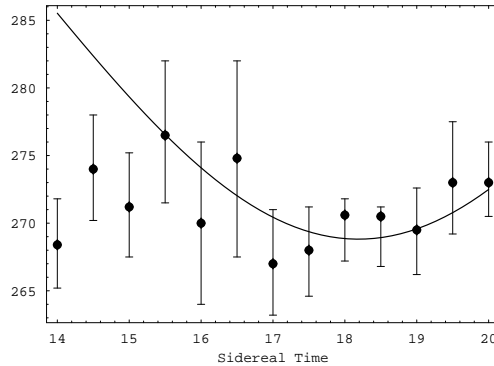


Figure 17: Frequency difference in kHz between the two masers in the 1963 New Bedford experiment after a  $90^0$  rotation. The 275kHz difference is a systematic repeatable apparatus effect, whereas the superimposed ‘dip’ at 17–18:00<sup>hr</sup> sidereal time of approximately 3kHz is a real time dependent frequency difference. The full curve shows the theoretical prediction for the time of the ‘dip’ for this experiment using the Miller direction for  $\hat{\mathbf{v}}$  ( $\alpha = 5.2^{hr}$ ,  $\delta = -67^0$ ) with  $|\mathbf{v}| = 433\text{km/s}$  and including the earth’s orbital velocity and sun gravitational in-flow velocity effects for January 20, 1963. The absolute scale of this theoretical prediction was not possible to compute as the refractive index of the He-Ne gas mixture was unknown.

because the Newtonian physics analysis gave the wrong prediction then Einstein relativity must be correct. But the analysis simply failed to take account of the Fitzgerald-Lorentz contraction, which had been known since the end of the 19<sup>th</sup> century, and the refractive index effect which had an even longer history. As well the authors failed to convert their local times to sidereal times and compare the time for the ‘dip’ with Miller’s time<sup>8</sup>.

### 3.9 The DeWitte Experiment: 1991

The Michelson-Morley, Illingworth, Miller, Joos and New Bedford experiments all used Michelson interferometers or its equivalent in gas mode, and all revealed absolute motion. The Michelson interferometer is a 2nd-order device meaning that the time difference between the ‘arms’ is proportional to  $(v/c)^2$ . There is also a factor of  $n^2 - 1$  and for gases like air and particularly helium or helium-neon mixes this results in very small time differences and so these experiments were always very difficult. Of course without the gas the Michelson interferometer is incapable of detecting absolute motion<sup>9</sup>, and so there are fundamental limitations to the use of this interferometer in the study of absolute motion and related effects.

In a remarkable development in 1991 a research project within Belgacom, the Belgium telecommunications company, stumbled across yet another detection of

<sup>8</sup>There is no reference to Miller’s 1933 paper in Ref.[14].

<sup>9</sup>So why not use a transparent solid in place of the gas? See Sect.3.14 for the discussion.

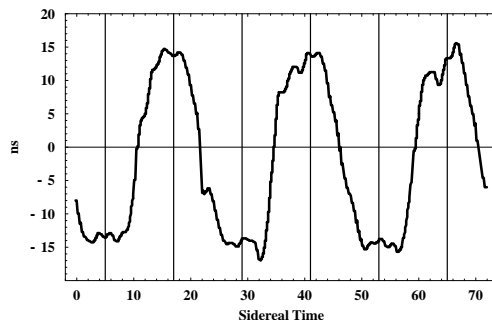


Figure 18: Variations in twice the one-way travel time, in ns, for an RF signal to travel 1.5 km through a coaxial cable between Rue du Marais and Rue de la Paille, Brussels. An offset has been used such that the average is zero. The definition of the sign convention for  $\Delta t$  used by DeWitte is unclear. The cable has a North-South orientation, and the data is  $\pm$  difference of the travel times for NS and SN propagation. The sidereal time for maximum effect of  $\sim 17$ hr (or  $\sim 5$ hr) (indicated by vertical lines) agrees with the direction found by Miller and also by Jaseja *et al*, but because of the ambiguity in the definition of  $\Delta t$  the opposite direction would also be consistent with this data. Plot shows data over 3 sidereal days and is plotted against sidereal time. See Fig.19b for theoretical predictions for one sidereal day. The time of the year of the data is not identified. The fluctuations are evidence of turbulence associated with the gravitational in-flow towards the sun. Adapted from DeWitte [16].

absolute motion, and one which turned out to be 1st-order in  $v/c$ . The study was undertaken by Roland DeWitte [16]. This organisation had two sets of atomic clocks in two buildings in Brussels separated by 1.5 km and the research project was an investigation of the task of synchronising these two clusters of atomic clocks. To that end 5MHz radiofrequency signals were sent in both directions through two buried coaxial cables linking the two clusters. The atomic clocks were caesium beam atomic clocks, and there were three in each cluster. In that way the stability of the clocks could be established and monitored. One cluster was in a building on Rue du Marais and the second cluster was due south in a building on Rue de la Paille. Digital phase comparators were used to measure changes in times between clocks within the same cluster and also in the propagation times of the RF signals. Time differences between clocks within the same cluster showed a linear phase drift caused by the clocks not having exactly the same frequency together with short term and long term noise. However the long term drift was very linear and reproducible, and that drift could be allowed for in analysing time differences in the propagation times between the clusters.

Changes in propagation times were observed and eventually observations over 178 days were recorded. A sample of the data, plotted against sidereal time for just three days, is shown in Fig.18. DeWitte recognised that the data was evidence of absolute motion but he was unaware of the Miller experiment and did not realise that the Right Ascension for maximum/minimum propagation time agreed almost exactly with Miller's direction  $(\alpha, \delta) = (5.2^h, -67^0)$ . In

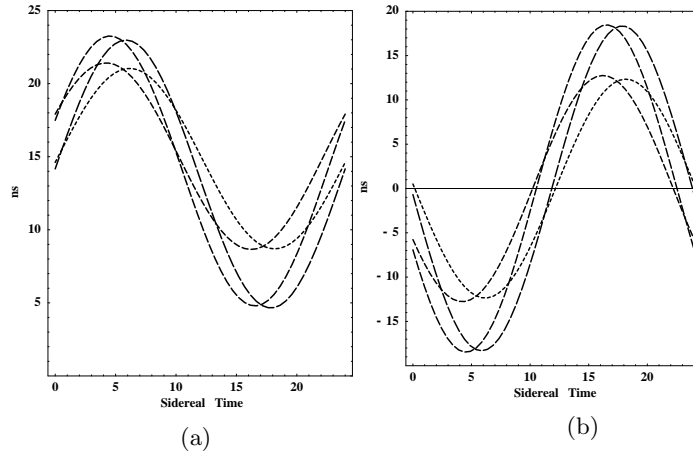


Figure 19: Theoretical predictions for the variations in travel time, in ns, for one sidereal day, in the DeWitte Brussels coaxial cable experiment for  $\mathbf{v}_{cosmic}$  in the direction  $(\alpha, \delta) = (5.2^h, -67^0)$  and with the Miller magnitude of 443 km/s, and including orbital and in-flow effects (but without turbulence). Shown are the results for four days: for the Vernal Equinox, March 21 (shortest dashes), and for 90, 180 and 270 days later (shown with increasing dash length). Figure (a) Shows change in one-way travel time  $t_{0nvP}/c$  for signal travelling from N to S. Figure (b) shows  $\Delta t$ , as defined in (76), with an offset such that the average is zero so as to enable comparison with the data in Fig.18.  $\Delta t$  is twice the one-way travel time. For the direction opposite to  $(\alpha, \delta) = (5.2^h, -67^0)$  the same curves arise except that the identification of the months is different and the sign of  $\Delta t$  also changes. The sign of  $\Delta t$  determines which of the two directions is the actual direction of absolute motion. However the definition of the sign convention for  $\Delta t$  used by DeWitte is unclear.

fact DeWitte expected that the direction of absolute motion should have been in the CMB direction, but that would have given the data a totally different sidereal time signature, namely the times for maximum/minimum would have been shifted by 6 hrs. The declination of the velocity observed in this DeWitte experiment cannot be determined from the data as only three days of data are available. However assuming exactly the same declination as Miller the speed observed by DeWitte appears to be also in excellent agreement with the Miller speed, which in turn is in agreement with that from the Michelson-Morley and Illingworth experiments, as shown in Fig.13.

Being 1st-order in  $v/c$  the Belgacom experiment is easily analysed to sufficient accuracy by ignoring relativistic effects, which are 2nd-order in  $v/c$ . Let the projection of the absolute velocity vector  $\mathbf{v}$  onto the direction of the coaxial cable be  $v_P$  as before. Then the phase comparators reveal the difference between the propagation times in NS and SN directions. Consider the analysis with no Fresnel drag effect,

$$\begin{aligned}\Delta t &= \frac{L}{\frac{c}{n} - v_P} - \frac{L}{\frac{c}{n} + v_P}, \\ &= 2\frac{L}{c/n}n\frac{v_P}{c} + O\left(\frac{v_P^2}{c^2}\right) \approx 2t_0n\frac{v_P}{c}.\end{aligned}\tag{76}$$

Here  $L = 1.5$  km is the length of the coaxial cable,  $n = 1.5$  is the refractive index of the insulator within the coaxial cable, so that the speed of the RF signals is approximately  $c/n = 200,000$ km/s, and so  $t_0 = nL/c = 7.5 \times 10^{-6}$  sec is the one-way RF travel time when  $v_P = 0$ . Then, for example, a value of  $v_P = 400$ km/s would give  $\Delta t = 30$ ns. Because Brussels has a latitude of  $51^\circ$  N then for the Miller direction the projection effect is such that  $v_P$  almost varies from zero to a maximum value of  $|\mathbf{v}|$ . The DeWitte data in Fig.18 shows  $\Delta t$  plotted with a false zero, but shows a variation of some 28 ns. So the DeWitte data is in excellent agreement with the Miller's data<sup>10</sup>. The Miller experiment has thus been confirmed by a non-interferometer experiment.

The actual days of the data in Fig.18 are not revealed in Ref.[16] so a detailed analysis of the DeWitte data is not possible. Nevertheless theoretical predictions for various days in a year are shown in Fig.19 using the Miller speed of  $v_{cosmic} = 433$  km/s and where the diurnal effects of the earth's orbital velocity and the gravitational in-flow cause the range of variation of  $\Delta t$  and sidereal time of maximum effect to vary throughout the year. The predictions give  $\Delta t = 30 \pm 4$  ns over a year compared to the DeWitte value of 28 ns in Fig.18. If all of DeWitte's 178 days of data were available then a detailed analysis would be possible.

Ref.[16] does however reveal the sidereal time of the cross-over time, that is a 'zero' time in Fig.18, for all 178 days of data. This is plotted in Fig.20 and demonstrates that the time variations are correlated with sidereal time and not

<sup>10</sup>There is ambiguity in Ref.[16] as to whether the time variations in Fig.18 include the factor of 2 or not, as defined in (76). It is assumed here that a factor of 2 is included.

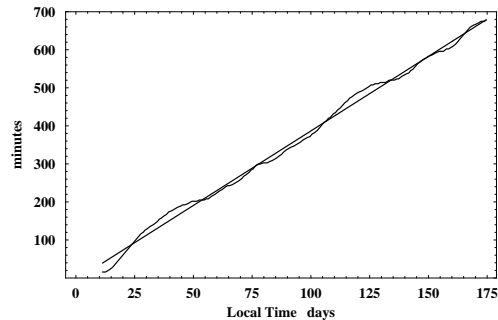


Figure 20: Plot of the negative of the drift of the cross-over time between minimum and maximum travel-time variation each day (at  $\sim 10^h \pm 1^h$  ST) versus local solar time for some 180 days. The straight line plot is the least squares fit to the experimental data, giving an average slope of 3.92 minutes/day. The time difference between a sidereal day and a solar day is 3.93 minutes/day. This demonstrates that the effect is related to sidereal time and not local solar time. The actual days of the year are not identified in Ref.[16]. Adapted from DeWitte [16].

local solar time. A least squares best fit of a linear relation to that data gives that the cross-over time is retarded, on average, by 3.92 minutes per solar day. This is to be compared with the fact that a sidereal day is 3.93 minutes shorter than a solar day. So the effect is certainly cosmological and not associated with any daily thermal effects, which in any case would be very small as the cable is buried. Miller had also compared his data against sidereal time and established the same property, namely that up to small diurnal effects identifiable with the earth's orbital motion, features in the data tracked sidereal time and not solar time; see Ref.[11] for a detailed analysis.

The DeWitte data is also capable of resolving the question of the absolute direction of motion found by Miller. Is the direction  $(\alpha, \delta) = (5.2^h, -67^0)$  or the opposite direction? By doing a 2nd-order Michelson interferometer experiment Miller had to rely on the earth's diurnal effects in order to resolve this ambiguity, but his analysis of course did not take account of the gravitational in-flow effect, and so until a re-analysis of his data his preferred choice of direction must remain to be confirmed. The DeWitte experiment could easily resolve this ambiguity by simply noting the sign of  $\Delta t$ . Unfortunately it is unclear in Ref.[16] as to how the sign in Fig.18 is actually defined, and DeWitte does not report a direction expecting, as he did, that the direction should have been the same as the CMB direction.

The DeWitte observations were truly remarkable considering that initially they were serendipitous. They demonstrated yet again that the Einstein postulates were in contradiction with experiment. To my knowledge no physics journal has published a report of the DeWitte experiment.

That the DeWitte experiment is not a gas-mode Michelson interferometer experiment is very significant. The value of the speed of absolute motion re-

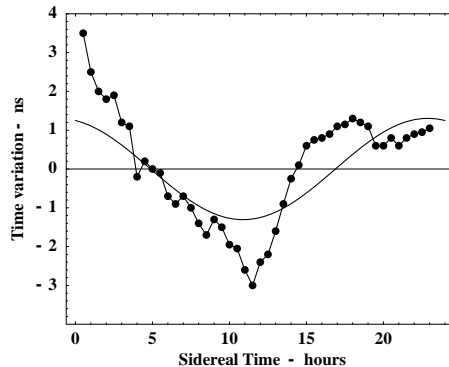


Figure 21: Data from the 1981 Torr-Kolen experiment at Logan, Utah [15]. The data shows variations in travel times (ns), for local times, of an RF signal travelling through 500m of coaxial cable orientated in an E-W direction. Actual days are not indicated but the experiment was done during February-June 1981. Results are for a typical day. For the 1st of February the local time of 12:00 corresponds to 13:00 sidereal time. The predictions are for February for a cosmic speed of 433 km/s in the direction  $(\alpha, \delta) = (5.2^h, -72^0)$ , and including orbital and in-flow velocities but without theoretical turbulence.

vealed by the DeWitte experiment of some 400 km/s is in agreement with the speeds revealed by the new analysis of various Michelson interferometer data, which used the recently discovered refractive index effect, see Fig.13. Not only was this effect confirmed by comparing results for different gases, but the re-scaling of the older  $v_M$  speeds to  $v = v_M/\sqrt{n^2 - 1}$  speeds resulting from this effect are now confirmed.

### 3.10 The Torr-Kolen Experiment: 1981

A coaxial cable experiment similar to but before the DeWitte experiment was performed at the University of Utah in 1981 by Torr and Kolen [15]. This involved two rubidium vapor clocks placed approximately 500m apart with a 5 MHz sinewave RF signal propagating between the clocks via a nitrogen filled coaxial cable maintained at a constant pressure of  $\sim 2$  psi. This means that the Fresnel drag effect is not important in this experiment. Unfortunately the cable was orientated in an East-West direction which is not a favourable orientation for observing absolute motion in the Miller direction, unlike the Brussels North-South cable orientation. There is no reference to Miller's result in the Torr and Kolen paper, otherwise they would presumably not have used this orientation. Nevertheless there is a projection of the absolute motion velocity onto the East-West cable and Torr and Kolen did observe an effect in that, while the round speed time remained constant within 0.0001% $c$ , typical variations in the one-way travel time were observed, as shown in Fig.21 by the data points. The theoretical predictions for the Torr-Kolen experiment for a cosmic speed of 433



km/s in the direction  $(\alpha, \delta) = (5.2^h, -67^0)$ , and including orbital and in-flow velocities, are shown in Fig.21. As well the maximum effect occurred, typically, at the predicted times. So the results of this experiment are also in remarkable agreement with the Miller direction, and the speed of 433 km/s which of course only arises after re-scaling the Miller speeds for the effects of the gravitational in-flow. As well Torr and Kolen reported fluctuations in both the magnitude and time of the maximum variations in travel time just as DeWitte observed some 10 years later. Again we argue that these fluctuations are evidence of genuine turbulence in the in-flow as discussed in Sect.3.12. So the Torr-Kolen experiment again shows strong evidence for the new theory of gravity, and which is over and above its confirmation of the various observations of absolute motion.

### 3.11 Galactic In-flow and the CMB Frame

Absolute motion (AM) of the solar system has been observed in the direction  $(\alpha, \delta) = (5.2^h, -67^0)$ , up to an overall sign to be sorted out, with a speed of 433 km/s. This is the velocity after removing the contribution of the earth's orbital speed and the sun in-flow effect. It is significant that this velocity is different to that associated with the Cosmic Microwave Background (CMB) relative to which the solar system has a speed of 369 km/s in the direction  $(\alpha, \delta) = (11.20^h, -7.22^0)$ , see [22]. This CMB velocity is obtained by finding the preferred frame in which this thermalised 3<sup>0</sup>K radiation is isotropic, that is by removing the dipole component. The CMB velocity is a measure of the motion of the solar system relative to the universe as a whole, or at least a shell of the universe some 15Gyrs away, and indeed the near uniformity of that radiation in all directions demonstrates that we may meaningfully refer to the spatial structure of the universe. The concept here is that at the time of decoupling of this radiation from matter that matter was on the whole, apart from small observable fluctuations, at rest with respect to the quantum-foam system that is space. So the CMB velocity is the motion of the solar system with respect to space *universally*, but not necessarily with respect to the *local* space. Contributions to this velocity would arise from the orbital motion of the solar system within the Milky Way galaxy, which has a speed of some 250 km/s, and contributions from the motion of the Milky Way within the local cluster, and so on to perhaps larger clusters.

On the other hand the AM velocity is a vector sum of this *universal* CMB velocity and the net velocity associated with the *local* gravitational in-flows into the Milky Way and the local cluster. If the CMB velocity had been identical to the AM velocity then the in-flow interpretation of gravity would have been proven wrong. We therefore have three pieces of experimental evidence for this interpretation (i) the refractive index anomaly discussed previously in connection with the Miller data, (ii) the turbulence seen in all detections of absolute motion, and now (iii) that the AM velocity is different in both magnitude and direction from that of the CMB velocity, and that this CMB velocity does not display the turbulence seen in the AM velocity.

That the AM and CMB velocities are different amounts to the discovery of the resolution to the ‘dark matter’ conjecture. Rather than the galactic velocity anomalies being caused by such undiscovered ‘dark matter’ we see that the in-flow into non spherical galaxies, such as the spiral Milky Way, will be non Newtonian. As well it will be interesting to determine, at least theoretically, the scale of turbulence expected in galactic systems, particularly as the magnitude of the turbulence seen in the AM velocity is somewhat larger than might be expected from the sun in-flow alone. Any theory for the turbulence effect will certainly be checkable within the solar system as the time scale of this is suitable for detailed observation.

It is also clear that the time of observers at rest with respect to the CMB frame is absolute or universal time. This interpretation of the CMB frame has of course always been rejected by supporters of the SR/GR formalism. As for space we note that it has a differential structure, in that different regions are in relative motion. This is caused by the gravitational in-flow effect locally, and as well by the growth of the universe.

### 3.12 In-Flow Turbulence and Gravitational Waves

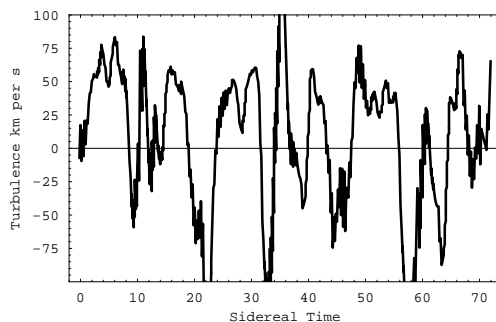


Figure 22: Speed fluctuations determined from Fig.18 by subtracting a least squares best fit of the forms shown in Fig.19b. A 1ns variation in travel time corresponds approximately to a speed variation of 27km/s. The larger speed fluctuations actually arise from a fluctuation in the cross-over time, that is, a fluctuation in the direction of the velocity. This plot implies that the velocity flow-field is turbulent. The scale of this turbulence is comparable to that evident in the Miller data, as shown in Fig.9 and Fig.23a.

The velocity flow-field equation is expected to have solutions possessing turbulence, that is, fluctuations in both the magnitude and direction of the gravitational in-flow component of the velocity flow-field. Indeed all the Michelson interferometer experiments showed evidence of such turbulence. The first clear evidence was from the Miller experiment, as shown in Figs.9 and 11. Miller offered no explanation for these fluctuations but in his analysis of that data he did running time averages. Miller may have in fact have simply interpreted these

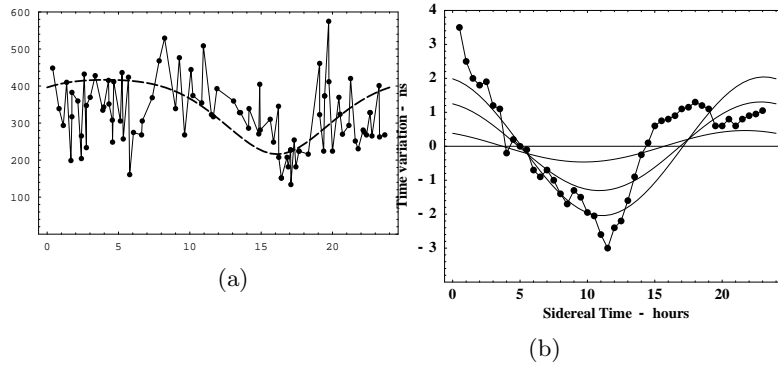


Figure 23: (a) The absolute projected speeds  $v_P$  in the Miller experiment plotted against sidereal time in hours for September 1925, showing the variations in speed caused by the gravitational wave turbulence. and (b) similar variations in travel times when the declination is varied by  $\pm 10^\circ$  about the direction  $\alpha = 5.2^\circ, \delta = -67^\circ$ , for a cosmic speed of 433 km/s in the Torr-Kolen experiment.

fluctuations as purely instrumental effects. While some of these fluctuations may be partially caused by weather related temperature and pressure variations, the bulk of the fluctuations appear to be larger than expected from that cause alone. Even the original Michelson-Morley data in Fig.8 shows variations in the velocity field and supports this interpretation. However it is significant that the non-interferometer DeWitte data also shows evidence of turbulence in both the magnitude and direction of the velocity flow field, as shown in Fig.22. Just as the DeWitte data agrees with the Miller data for speeds and directions the magnitude fluctuations, shown in Fig.22, are very similar in absolute magnitude to, for example, the Miller speed turbulence shown in Fig.23a. As well the orientation of the Torr-Kolen coaxial cable is very sensitive to the directional changes associated with the turbulence. Being almost at  $90^\circ$  to the direction of absolute motion, any variation in that direction produces significant effects, as shown in Fig. 23b where the declination is varied by  $\pm 10^\circ$ . Indeed Torr and Kolen [15] reported significant fluctuations in the coaxial cable travel times from day to day, as expected.

It therefore becomes clear that there is strong evidence from these three experiments for these fluctuations being evidence of physical turbulence in the flow field. The magnitude of this turbulence appears to be somewhat larger than that which would be caused by the in-flow of quantum foam towards the sun, and indeed following on from Sect.3.11 some of this turbulence may be associated with galactic in-flow into the Milky Way. This in-flow turbulence is a form of gravitational wave and the ability of gas-mode Michelson interferometers to detect absolute motion means that experimental evidence of such a wave phenomena has been available for a considerable period of time, but suppressed along with the detection of absolute motion itself. Of course flow equations of the form (47) do not exhibit those gravitational waves of the form that have

been predicted to exist based on the Einstein equations, and which are supposed to propagate at the speed of light. All this means that gravitational wave phenomena are very easy to detect and amount to new physics that can be studied in much detail.

### 3.13 Vacuum Michelson Interferometers

Over the years vacuum-mode Michelson interferometer experiments have become increasingly popular, although the motivation for such experiments appears to be increasingly unclear. The first vacuum interferometer experiment was planned by Joos [13] in 1930, but because of technical problems helium was actually used, as discussed in section 3.7. The first actual vacuum experiment was by Kennedy and Thorndike [18]. The result was actually unclear but was consistent with a null effect as predicted by both the quantum-foam physics and the Einstein physics. Only Newtonian physics is disproved by such experiments. These vacuum interferometer experiments do give null results, with increasing confidence level, as for example in Refs.[18, 19, 20, 21], but they only check that the Lorentz contraction effect completely cancels the geometrical path-length effect in vacuum experiments, and this is common to both theories. So they are unable to distinguish the new physics from the Einstein physics. Nevertheless recent works [20, 21] continue to claim that the experiment had been motivated by the desire to look for evidence of absolute motion, despite effects of absolute motion having been discovered as long ago as 1887. The ‘null results’ are always reported as proof of the Einstein formalism. Unfortunately the analysis of the data from such experiments is always by means of the Robertson [67] and Mansouri and Sexl formalism [68], which purports to be a generalisation of the Lorentz transformation if there is a preferred frame. However we have seen that absolute motion effects, that is the existence of a preferred frame, are consistent with the usual Lorentz transformation, based as it is on the restricted Einstein measurement protocol. A preferred frame is revealed by gas-mode Michelson interferometer experiments, and then the refractive index of the gas plays a critical role in interpreting the data. The Robertson and Mansouri-Sexl formalism contains no contextual aspects such as a refractive index effect and is thus totally inappropriate to the analysis of so called ‘preferred frame’ experiments.

It is a curious feature of the history of Michelson interferometer experiments that it went unnoticed that the results fell into two distinct classes, namely vacuum and gas-mode, with recurring non-null results from gas-mode interferometers.

### 3.14 Solid-State Michelson Interferometers

The gas-mode Michelson interferometer has its sensitivity to absolute motion effects greatly reduced by the refractive index effect, namely the  $k^2 = n^2 - 1$  factor in (62), and for gases with  $n$  only slightly greater than one this factor has caused much confusion over the last 115 years. So it would be expected

that passing the light beams through a transparent solid with  $n \approx 1.5$  rather than through a gas would greatly increase the sensitivity. Such an Michelson interferometer experiment was performed by Shamir and Fox [69] in Haifa in 1969. This interferometer used light from a He-Ne laser and used perspex rods with  $L = 0.26\text{m}$ . The experiment was interpreted in terms of the supposed Fresnel drag effect, which has a drag coefficient given by  $b = 1 - 1/n^2$ . The light passing through the solid was supposed to be ‘dragged’ along in the direction of motion of the solid with a velocity  $\Delta\mathbf{V} = b\mathbf{v}$  additional to the usual  $c/n$  speed. As well the Michelson geometrical path difference and the Lorentz contraction effects were incorporated into the analysis. The outcome was that no fringe shifts were seen on rotation of the interferometer, and Shamir and Fox concluded that this negative result “*enhances the experimental basis of special relativity*”.

The Shamir-Fox experiment was unknown to us<sup>11</sup> at Flinders university when in 2002 several meters of optical fibre were used in a Michelson interferometer experiment which also used a He-Ne laser light source. Again because of the  $n^2 - 1$  factor, and even ignoring the Fresnel drag effect, one would have expected large fringe shifts on rotation of the interferometer, but none were observed. As well in a repeat of the experiment single-mode optical fibres were also used and again with no rotation effect seen. So this experiment is consistent with the Shamir-Fox experiment. Re-doing the analysis by including the supposed Fresnel drag effect, as Shamir and Fox did, makes no material difference to the expected outcome. In combination with the non-null results from the gas-mode interferometer experiments along with the non-interferometer experiment of DeWitte it is clear that transparent solids behave differently to a gas when undergoing absolute motion through the quantum foam. Indeed this in itself is a discovery of a new phenomena.

The most likely explanation is that the physical Fitzgerald-Lorentz contraction effect has a anisotropic effect on the refractive index of the transparent solid, and this is such as to cause a cancellation of any differences in travel time between the two arms on rotation of the interferometer. In this sense a transparent solid medium shares this outcome with the vacuum itself.

### 3.15 Absolute Motion and Quantum Gravity

Absolute rotational motion had been recognised as a meaningful and observable phenomenon from the very beginning of physics. Newton had used his rotating bucket experiment to illustrate the reality of absolute rotational motion, and later Foucault and Sagnac provided further experimental proof. But for absolute linear motion the history would turn out to be completely different. It was generally thought that absolute linear motion was undetectable, at least until Maxwell’s electromagnetic theory appeared to require it. In perhaps the most bizarre sequence of events in modern science it turns out that absolute linear motion has been apparent within experimental data for over 100 years. It was

---

<sup>11</sup>This experiment was performed by Professor Warren Lawrance, an experimental physical chemist with considerable laser experience.

missed in the first experiment designed to detect it and from then on for a variety of sociological reasons it became a concept rejected by physicists and banned from their journals despite continuing new experimental evidence. Those who pursued the scientific evidence were treated with scorn and ridicule. Even worse was the impasse that this obstruction of the scientific process resulted in, namely the halting of nearly all progress in furthering our understanding of the phenomena of gravity. For it is clear from all the experiments that were capable of detecting absolute motion that there is present in that data evidence of turbulence within the velocity field. Both the in-flow itself and the turbulence are manifestations at a classical level of what is essentially quantum gravity processes, for these processes imply that space has structure.

Process Physics has given a unification of explanation and description of physical phenomena based upon the limitations of formal syntactical systems which had nevertheless achieved a remarkable encapsulation of many phenomena, albeit in a disjointed and confused manner, and with a dysfunctional ontology attached for good measure. As argued in [2] space is a quantum system continually classicalised by on-going non-local collapse processes. The emergent phenomenon is foundational to existence and experientialism. Gravity in this system is caused by differences in the rate of processing of the cellular information within the network which we experience as space, and consequentially there is a differential flow of information which can be affected by the presence of matter or even by space itself. Of course the motion of matter including photons with respect to that spatial information content is detectable because it affects the geometrical and chronological attributes of that matter, and the experimental evidence for this has been exhaustively discussed above. What has become very clear is that the phenomenon of gravity is only understandable once we have this unification of the quantum phenomena of matter and the quantum phenomenon of space itself. In Process Physics the difference between matter and space is subtle. It comes down to the difference between informational patterns that are topologically preserved and those information patterns that are not. One outcome of this unification is that as a consequence of having a quantum phenomenon of space itself we obtain an informational explanation for gravity, and which at a suitable level has an emergent quantum description. In this sense we have an emergent quantum theory of gravity. Of course no such quantum description of gravity is derivable from quantising Einsteinian gravity itself. This follows on two counts, one is that the Einstein gravity formalism fails on several levels, as discussed previously, and second that quantisation has no validity as a means of uncovering deeper physics. Most surprising of all is that having uncovered the logical necessity for gravitational phenomena it also appears that even the seemingly well-founded Newtonian account of gravity has major failings. The denial of this possibility has resulted in an unproductive search for dark matter. Indeed like dark matter and spacetime much of present day physics has all the hallmarks of another episode of Ptolemy's epicycles, namely concepts that appear to be well founded but in the end turn out to be illusions, and ones that have acquired the status of dogma.

If the Michelson-Morley experiment had been properly analysed and the

phenomena revealed by the data exposed, and this would have required in 1887 that Newtonian physics be altered, then as well as the subsequent path of physics being very different, physicists would almost certainly have discovered both the gravitational in-flow effect and associated gravitational waves.

It is clear then that observation and measurement of absolute motion leads directly to a changed paradigm regarding the nature and manifestations of gravitational phenomena. There are two aspects of such an experimental program. One is the characterisation of the turbulence and its linking to the new non-linear term in the velocity field theory. This is a top down program. The second aspect is a bottom-up approach where the form of the velocity field theory, or its modification, is derived from the deeper informational process physics. This is essentially the quantum gravity route. The turbulence is of course essentially a gravitational wave phenomena and networks of 1st-order interferometers will permit spatial and time series analysis. There are a number of other gravitational anomalies which may also now be studied using such an interferometer network, and so much new physics can be expected to be uncovered.

## 4 Conclusions

We have shown here that seven experiments, so far, have clearly revealed experimental evidence of absolute motion. As well these are all consistent with respect to the direction and speed of that motion. This clearly refutes the fundamental postulates of the Einstein reinterpretation of the relativistic effects that had been developed earlier by Lorentz and others. Indeed these experiments are consistent with the Lorentzian interpretation of the special relativistic effects in which reality displays both absolute motion and relativistic effects. It is absolute motion that actually causes these relativistic effects. Data from the five Michelson interferometer fringe-shift experiments had never been properly analysed until now. That analysis requires that the Fitzgerald-Lorentz contraction effect be taken into account, as well as the effect of the gas on the speed of light in the interferometer. Only then does the fringe-shift data from air and helium interferometer experiments become consistent, and then also consistent with the two RF coaxial cable travel-time experiments. The seasonal changes in the Miller fringe-shift data reveal the orbital motion of the earth about the sun, as well as an in-flow of space past the earth into the sun. These results support the new theory of gravity. As well the large cosmic velocity of the solar system is seen to be different to the velocity associated with the Cosmic Microwave Background, which implies another gravitational in-flow, this time into the Milky Way and Local Cluster. The fringe-shift data has also indicated the presence of turbulence in these gravitational in-flows, and this amounts to the detection of gravitational waves. These are waves predicted by the new theory of gravity, and not those associated with the Hilbert-Einstein theory of gravity. As noted the Newtonian theory of gravity is deeply flawed, as revealed by its inability to explain a growing number of gravitational anomalies, but which are

explained by the new theory. These flaws arose because the solar system was too special, because of its high spherical symmetry, to have revealed the full range of phenomena that is gravity. General Relativity ‘inherited’ these flaws, and so is itself flawed. As discussed the clear-cut checks of General Relativity were actually done in systems also with high spherical symmetry.

Here a new theory of gravity has been proposed. It passes all the key existing tests, including the operation of the GPS, and also appears to be capable of explaining numerous gravitational anomalies. The phenomena present in these anomalies provide opportunities for further tests of the new gravitational physics, as illustrated here by the mine/borehole  $g$  anomaly. This new theory explains why elliptical galaxies display a very small ‘dark matter’ effect, in comparison with the large effect for the spiral galaxies. This new theory is supported by the Miller, Torr and Kolen, and DeWitte absolute motion experiments in that they reveal the turbulent in-flow of space associated with gravity, namely the discovery of those gravitational waves predicted by the new theory, as well as the existence of absolute motion itself.

The experiments are consistent with the Lorentzian interpretation of the special relativistic effects in that reality displays both absolute motion effects *and* relativistic effects. It is absolute motion that causes the special relativistic effects. We saw that the Galilean transformation together with the absolute motion effects of time dilations and length contractions for moving matter systems leads to the data from observers in absolute motion being related by the Lorentz transformation, so long as their data are not corrected for the effects of absolute motion. So the new Process Physics brings together transformations that were, in the past, regarded as mutually exclusive. Essentially the quantum foam system that is space generates phenomena that are more subtle than currently considered in physics. Discussed in [1, 2] was an explanation for the ‘dark energy’ phenomena, previously known as the cosmological constant, associated with the accelerating rate of expansion of the universe - that also is seen to be a consequence of the information theoretic aspects of the quantum foam.

## 5 Acknowledgments

Special thanks to Professor Warren Lawrance, Professor Igor Bray, Dr Ben Varcoe and Dr Lance McCarthy. Thanks to Katie Pilypas for running the codes to fit the Miller data.

## References

- [1] Process Physics URL:  
[http://www.scieng.flinders.edu.au/cpes/people/cahill\\_r/processphysics.html](http://www.scieng.flinders.edu.au/cpes/people/cahill_r/processphysics.html)



- [2] R.T. Cahill, *Process Physics: Inertia, Gravity and the Quantum*, *Gen. Rel. and Grav.* **34**, 1637-1656(2002); gr-qc/0110117.
- [3] R.T. Cahill, *Gravity as Quantum Foam In-Flow*, to be published in *Apeiron*; physics/0307003.
- [4] R.T. Cahill, *Absolute Motion and Gravitational Effects*, to be published in *Apeiron*; physics/0306196.
- [5] R.T. Cahill and C.M. Klinger, *Self-Referential Noise and the Synthesis of Three-Dimensional Space*, *Gen. Rel. and Grav.* **32**, (3)(2000), 529(2000); gr-qc/9812083.
- [6] R.T. Cahill, C.M. Klinger, *Self-Referential Noise as a Fundamental Aspect of Reality*, Proc. 2nd Int. Conf. on Unsolved Problems of Noise and Fluctuations (UPoN'99), Eds. D. Abbott and L. Kish, Adelaide, Australia, 11-15th July 1999, **Vol. 511**, p. 43 (American Institute of Physics, New York, 2000); gr-qc/9905082.
- [7] R.T. Cahill, C.M. Klinger, and K. Kitto, *Process Physics: Modelling Reality as Self-Organising Information*, *The Physicist* **37**(6), 191(2000); gr-qc/0009023.
- [8] R.T. Cahill and K. Kitto, *Michelson-Morley Experiments Revisited and the Cosmic Background Radiation Preferred Frame*, *Apeiron* **10**, No.2. 104-117(2003); physics/0205070.
- [9] M. Chown, *Random Reality*, *New Scientist*, Feb 26, **165**, No 2227, 24-28(2000).
- [10] A.A. Michelson and E.W. Morley, *Philos. Mag. S.5*, **24**, No. 151, 449-463(1887).
- [11] D.C. Miller, *The Ether-Drift Experiment and the Determination of the Absolute Motion of the Earth*, *Rev. Mod. Phys.* **5**, 203-242(1933).
- [12] K.K. Illingworth, *Phys. Rev.* **30**, 692-696(1927).
- [13] G. Joos, *Ann. d. Physik* [5], **7**, 385(1930).
- [14] T.S. Jaseja, A. Javan, J. Murray and C.H. Townes, *Test of Special Relativity or Isotropy of Space by Use of Infrared Masers*, *Phys. Rev. A* **133**, 1221(1964).
- [15] D.G. Torr and P. Kolen, *Precision Measurements and Fundamental Constants*, B.N. Taylor and W.D. Phillips, Eds. *Natl. Bur. Stand.(U.S.), Spec. Publ.* 617, 675(1984).
- [16] R. DeWitte, <http://www.ping.be/~pin30390/>, (1991).
- [17] A.A. Michelson, *Amer. J. Sci. S.* **3 22**, 120-129(1881).

- [18] H.P. Kennedy and E.M. Thorndike, *Phys. Rev.* **42**, 400(1932).
- [19] A. Brilliet and J.L. Hall, *Phys. Rev. Lett.* **42**, No.9, 549-552(1979).
- [20] C. Braxmaier, H. Müller, O. Prادل, J. Mlynek, A. Peters and S. Schiller, *Phys. Rev. Lett.* **88**, 010401(2002).
- [21] J.A. Lipa, J.A. Nissen, S. Wang, D.A. Striker and D. Avaloff, *Phys. Rev. Lett.* **90**, 060403-1(2003).
- [22] C. Lineweaver et al., *Astrophysics J.* **470**, 38(1996).
- [23] P. Panlevé, *C. R. Acad. Sci.*, **173**, 677(1921).
- [24] A. Gullstrand, *Ark. Mat. Astron. Fys.*, **16**, 1(1922).
- [25] W.M. Hicks, *Phil. Mag.*, [**6**], 3, 256(1902) ; 9, 555(1902) .
- [26] N. Ashby *Relativity in the Global Positioning System, Living Reviews in Relativity*, January 2003; [www.livingreviews.org/Articles/Volume6/2003-1Ashby](http://www.livingreviews.org/Articles/Volume6/2003-1Ashby).
- [27] P.R. Heyl and P. Chrzanowski, *J. Res. Nat. Bur. Standards* **29**, 1(1942).
- [28] L. Facy and C. Pontikis, *Comptes Rendus des Scéances de l'Académie des Sciences de Paris* **272**, Série B, 1397(1971).
- [29] J. Renner, in *Determination of Gravity Constant and Measurement of Certain Fine Gravity Effects*, Y. D. Boulanger and M. U. Sagitov (Eds.), (National Aeronautics and Space Administration, Washington, 1974), pp.26-31
- [30] M.U. Sagitov *et al.*, *Dok. Acad. Nauk SSSR* **245**, 567(1979).
- [31] G.G. Luther and W. Towler, *Phys. Rev. Letters* **48**, 121(1982).
- [32] J.-Cl. Dousse and Ch. Rhême, *Am. J. Phys.* **55**, 706(1987).
- [33] H. de Boer, H. Haars and W. Michaelis, *Metrologia* **24**, 171(1987).
- [34] M.A. Zumberge *et al.*, *J. Geophys. Res.* **95**, 15483(1990).
- [35] A. Cornaz, B. Hubler and W. Kündig, *Phys. Rev. Lett.* **72**, 1152(1994).
- [36] B. Hubler, A. Cornaz and W. Kündig, *Phys. Rev.* **D51**, 4005(1995).
- [37] M.P. Fitzgerald and T.R. Armstrong, *IEEE Trans. Instrum. Meas.* **44**, 494(1995).
- [38] C.H. Bagley and G.G. Luther, *Phys. Rev. Lett.* **78**, 3047(1997).
- [39] J. Luo *et al.*, *Phys. Rev.* **D59**, 042001(1998).
- [40] J. P. Schwarz *et al.*, 1998, *Science* **282**, 2230(1998).

- [41] O.V. Karagioz, V.P. Izmaylov and G.T. Gillies, *Grav. Cosmol.* **4**, 239(1998).
- [42] J. Schurr, F. Nolting and W. Kündig, *Phys. Rev. Letters* **80**, 1142(1998).
- [43] M.P. Fitzgerald and T.R. Armstrong, *Meas. Sci. Technol.* **10**, 439(1999).
- [44] F. Nolting, J. Schurr, S. Schlamminger and W. Kündig, *Meas. Sci. Technol.* **10**, 487(1999).
- [45] S.J. Richman, T.J. Quinn, C.C. Speake and R.S. Davis, *Meas. Sci. Technol.* **10**, 460(1999).
- [46] U. Kleinevoss, H. Meyer, A. Schumacher and S. Hartmann, *Meas. Sci. Technol.* **10**, 492(1999).
- [47] J. H.Gundlach and S.M. Merkowitz, *Phys. Rev. Letters* **85**, 2869(2000) and SISSA preprint gr-qc/0006043.
- [48] T.J. Quinn, C. C. Speake, S. J. Richman, R. S. Davis and A. Picard, *Phys. Rev. Lett.* **87**, 111101(2001).
- [49] P. Baldi *et al.*, *Phys. Rev.* **D64**, 082001(2001).
- [50] J.P. Mbelek and M. Lachièze-Rey, *Grav. Cosmol.* **8**331-338(2002).
- [51] G.T. Gillies, *The Newtonian Gravitational Constant: Recent Measurements and Related Studies, Rep. Prog. Phys.* **60**, 151-225(1997).
- [52] L. Swenson, *The Ethereal Aether: A History of the Michelson-Morley-Miller Aether Drift Experiments*, (U. Texas Press, Austin, 1972).
- [53] M. Allais, *AeroSpace Eng.*, Sept.-Oct. **18**, p.46(1959); <http://allais.maurice.free.fr/English/Science.htm>
- [54] E.J Saxl and M. Allen, *1970 Solar Eclipse as "Seen" by a Torsional Pendulum*, *Phys. Rev.*, **D3**, 823(1971).
- [55] S.W. Zhou and B.J. Huang, *Abnormalities of the Time Comparisons of Atomic Clocks during the Solar Eclipses*, *Il Nuovo Cimento*, **15C**, N.2, 133(1992).
- [56] S.W. Zhou and B.J. Huang, *Abnormalities of the Time Comparisons of Atomic Clocks during the Solar Eclipses*, *Il Nuovo Cimento*, **15C**, N.2, 133(1992).
- [57] S.W. Zhou, B.J. Huang and Z.M. Ren, *The Abnormal Influence of the Partial Solar Eclipse on December 24th, 1992, on the Time Comparisons between Atomic Clocks*, *Il Nuovo Cimento*, **18C**, N.2, 223(1995).
- [58] A.J. Romanowsky, *et al.*, *A Dearth of Dark Matter in Ordinary Elliptical Galaxies*, *Science*, **301**, 1696(2003).

- [59] J.D. Anderson, *et al.*, *Phys. Rev. Lett.* **81**, 2858(1998).
- [60] F.D. Stacey *et al.*, *Phys. Rev.* **D23**, 2683(1981).
- [61] S.C. Holding, F.D. Stacey, and G.J. Tuck, *Phys. Rev.* **D33**, 3487(1986).
- [62] S.C. Holding and G.J. Tuck, *Nature (London)* **307**, 714(1987).
- [63] F.D. Stacey, G.J.Tuck, G.I. More, S.C. Holding, B.D. Goodwin and R. Zhou, *Geophysics and the Law of Gravity, Rev. Mod. Phys.* **59**, 157(1987).
- [64] J. Thomas, *et al.*, *Testing the Inverse-Square Law of Gravity on a 465-m Tower, Phys. Rev. Lett.*, **63**, 1902(1989).
- [65] C. Jekeli, D.H. Eckhardt, and A.J. Romaides, *Phys. Rev. Lett.* **64**, 1204(1990).
- [66] E.G. Adelberger, *et al.*, *Ammu. Rev. Nucl. Part. Sci.*, **41**, pp. 269-320(1991).
- [67] H.P. Robertson, *Rev. Mod. Phys.*, **21**, 378(1949).
- [68] R.M. Mansouri and R.U. Sexl, *J. Gen. Rel. Grav.*, **8**, 497(1977), **8**, 515(1977), **8**, 809(1977).
- [69] J. Shamir and R. Fox, *Il Nuovo Cimenta*, **LXII B** N.2, 258(1969).